Responses to referee #1:

General comments: In the manuscript 'Understanding Climate-Fire-Ecosystem Inter- actions Using CESM-RESFire and Implications for Decadal Climate Variability', Zou et al. explored complex interactions between climate change, fire, and ecosystem using a global Earth System Model equipped with a coupled fire module. They estimated the global net radiative effects and NEE changes due to fire aerosols and fire-induced land cover changes under present-day and future scenarios. The topic is interesting and relevant to the scope of ACP. Overall, this is a nicely written manuscript with a clear description of data, model design and results. I recommend it to be published after some minor modifications suggested below.

Response: Thank you for your recommendation and constructive comments. We revised the manuscript accordingly to improve the presentation quality. Please see below the point-by-point responses and corresponding revisions in the manuscript.

Specific comments: My only major concern is the present manuscript lacks a detailed discussion about the uncertainty of the simulations and calculations. Specifically, although most current state-of-art fire models (including RESFire used in this study) may be able to reproduce the main spatial variability of fire emissions (and fire pollutants) under current climate condition, their ability to simulate temporal variability, as well as the changes under a changing climate has not been validated. As mentioned by the authors, some important processes (such as the lightning changes in the warming future) are also ignored in this study. It will be interesting to know how does it lead to changes in the simulated fire impacts in the future scenario. I believe this paper will be benefited from adding some discussions on this topic.

Response: Thank you for the helpful suggestion. We agree with you that uncertainty is still a challenging issue for the current state-of-art fire models. The same statement also applies to global lightning projections under climate change scenarios. Before using the RESFire model for future projections, we comprehensively evaluated its modeling performance in terms of both spatial distributions and temporal variations for global burned area and fire emissions in our previously published model development paper in the Journal of Advances in Modeling Earth Systems (JAMES, Zou et al., 2019). As shown in the following figures (Figs. R1 and R2) reproduced from Figs. 9 and 10 of Zou et al. (2019), the RESFire model captures the burning patterns and fire seasonality in different regions driven by either reanalysis-based atmospheric data (RESFire_CRUNCEP) or online simulated atmospheric data (RESFire_CAM5). It can also reproduce the observed decadal trends driven by different forcing factors such as decadal climate variability as well as demographic and socioeconomic changes as shown in Andela and van der Werf (2014) and Andela et al. (2017). However, since climate-fire-ecosystem interactions are of interest in this work, we fixed the socioeconomic factors such as population density and GDP in the RESFire simulations to eliminate the uncertainties associated with future population and socioeconomic projections. Lightning was also fixed in the future projections due to large uncertainty in its parameterization and future projections (Tost et al., 2007; Clark et al., 2017). There are other considerable uncertainty factors remaining in the projections, including fire emission estimation, fire radiative forcing related with aerosol-cloud interactions, fire induced land cover change and biogeochemical/biophysical effects, etc. We added a new section 3.4 to discuss the relevant uncertainties you suggested.

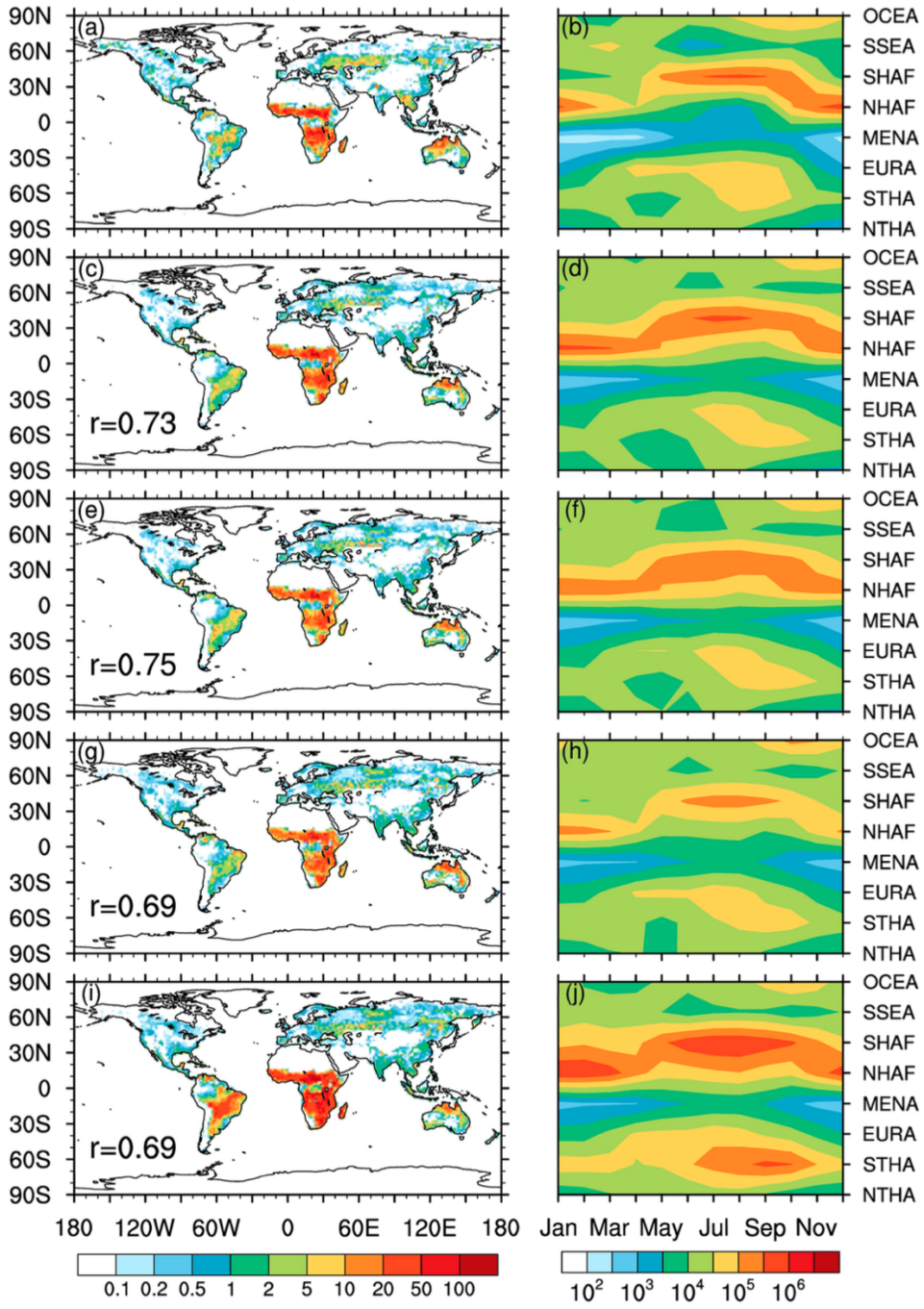

Figure R1 Comparisons of spatial distributions and seasonal variations of burned area in the observations and simulations. (a) GFED4.1s burned area fractions (%) averaged from 1997 to 2010; (b) seasonal variations of averaged GFED4.1s burned areas (km^2) in the eight subregions; (c, d) same as (a, b) but from RESFire_CRUNCEPa driven by the CRUNCEP reanalysis-based atmospheric data and varying population density; (e, f) same as (a, b) but from RESFire_CRUNCEPb driven by the CRUNCEP reanalysis-based atmospheric data and fixed population density; (g, h) same as (a, b) but from RESFire_CAM5a driven by online bias corrected CAM5 atmosphere simulations and fixed population density; (i, j) same as (a, b) but from RESFire_CAM5b driven by online CAM5 atmosphere simulations without bias correction and fixed population density. The spatial correlation coefficients between simulated global burned area fractions and the GFED4.1s data are shown on the bottom left corners of (c), (e), (g), and (i). RESFire = REgion-Specific ecosystem feedback Fire; GFED = Global Fire Emissions Database; CRUNCEP = Climatic Research Unit and National Centers for Environmental Prediction; CAM5 = Community Atmosphere Model version 5. (reproduced from Fig. 9 in Zou et al., 2019)

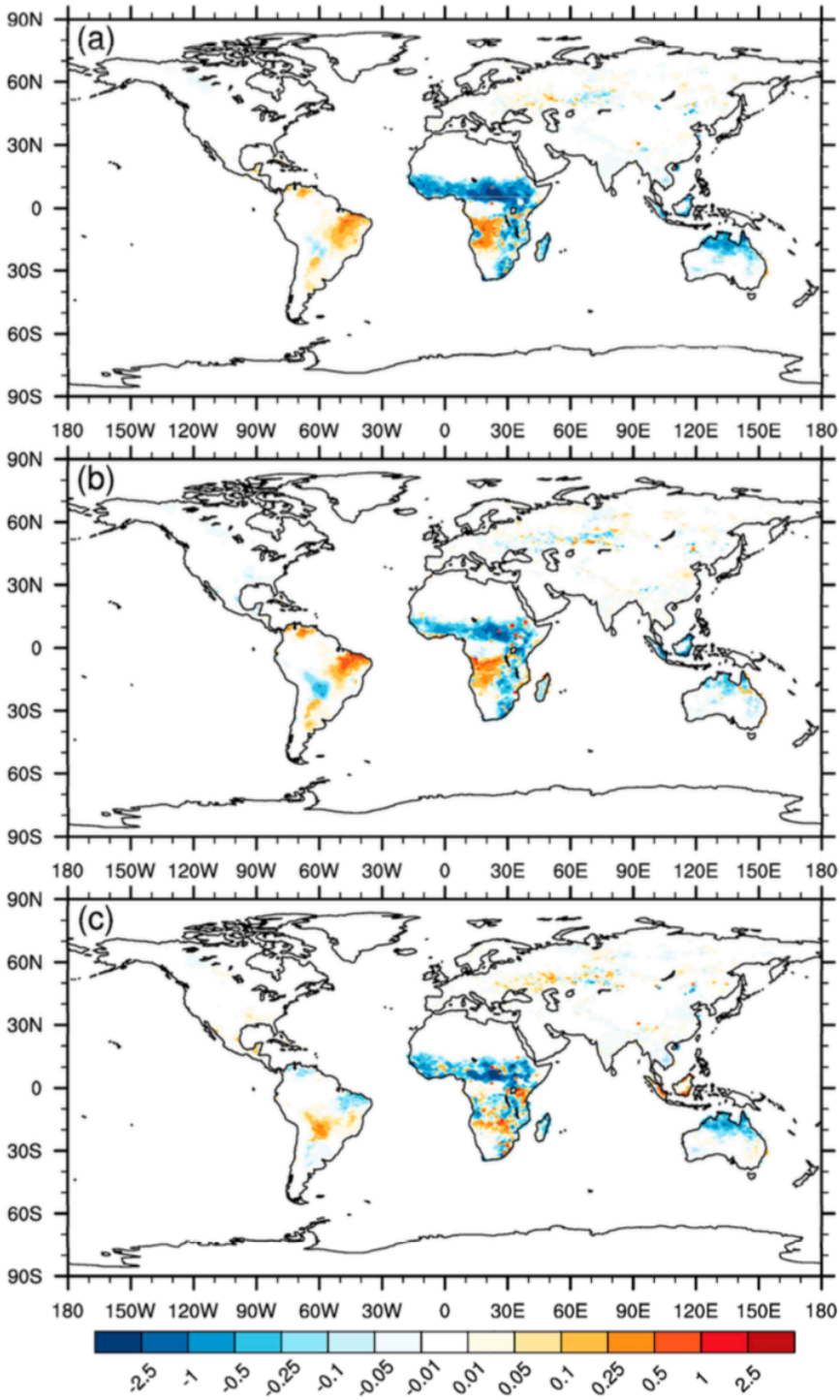

Figure R2 Comparisons of decadal trends (%/year) in annual averaged burned areas from 1991 to 2010. (a) Burned area trends driven by natural and demographic forcing in RESFire_CRUNCEPa with changing weather and population; (b) burned area trends driven by only natural forcing in RESFire_CRUNCEPb with changing weather but fixed population density; (c) burned area trends driven by demographic changes only. RESFire = REgion- Specific ecosystem feedback Fire; CRUNCEP = Climatic Research Unit and National Centers for Environmental Prediction. (reproduced from Fig. 10 in Zou et al., 2019)

Minor and technical comments:
Page 1, Line 17: "The complex climate-fire-ecosystem interactions were not included in previous climate model studies". I suggest softening the tune here. Some components of the interactions between climate, fire, and ecosystem have been considered in previous studies (although they were not necessarily incorporated into, or might not be represented thoroughly in a fully coupled online model).
Response: Thank you for the suggestion. We revised the narrative here to "The complex climate-fire-ecosystem interactions were not fully integrated in previous climate model studies".

Page 2, Line 58: "These processes were not included in previous climate model studies". Similar to the above, this sentence is way too assertive.
Response: Thank you. We revised it to "These processes were not fully included in previous climate model studies".

Page 3, Line 102-103: Since the new scheme is not implemented in this study (and the readers don't know the strength of the new approach), you don't have to mention it here. Removing this sentence won't affect the integrity of this paper.
Response: Thank you. The fire plume parameterization paper has been submitted to the Journal of Advances in Modeling Earth Systems and is under review now.

Page 7, Line 218-220: In addition to biogenic organic aerosols, can an underestimation of fire emissions be another reason for low simulated aerosols?
Response: You are right. We added this possible cause of underestimated fire emissions in line 231-232 of the revised manuscript as follows:
"Another possible cause for the underestimation problem is underrepresented burning activity due to deforestation and forest degradation and consequently underestimated fire aerosols emissions in these regions".
More detailed discussion is given in the next paragraph based on Fig. 2.

Page 7, Line 246-247: Any physical explanation for the differences between the signs of aerosol-cloud interactions and aerosol-radiation interactions?
Response: As explained in line 252-256, the land-sea contrast warming and cooling effects by aerosol-radiation interactions over Africa and South America (Fig. 3a) result from strong light absorption of fire aerosols enhanced by increased low-level cloud reflection over the downwind ocean areas. Fig. R3 shows the changes in low-level cloud fractions induced by fire aerosols in the present-day simulation (CTRL1-SENS1A). It demonstrates decreased low-level clouds over the African land region where biomass burning occurs and increased low-level clouds over the downwind Atlantic Ocean region. Therefore, opposite land-sea contrast signs occur due to distinct aerosol-cloud and aerosol-radiation interactions with positive aerosol-cloud radiative forcing over the land region and negative aerosol-cloud radiative forcing over the ocean area (Fig. 3b).

We added Fig. R3 in the supplement and more detailed explanation in line 259-265:
"The land-sea contrast of radiative effects emerges again in the vicinity of Africa and South America, but the signs of the contrasting effect related with aerosol-cloud interactions are opposite to these from aerosol-radiation interactions. The large amounts of fire aerosols suppress

low-level clouds over the African land region by stabilizing the lower atmosphere through reduction of radiative heating of the surface. However, fire aerosols increase cloud cover and brightness in the downwind Atlantic Ocean areas because they increase the number of cloud condensation nuclei and the larger cloud droplet number density reduce cloud droplet sizes (Lu et al., 2018; Rosenfeld et al., 2019; Fig. S1 in the Supplement)".

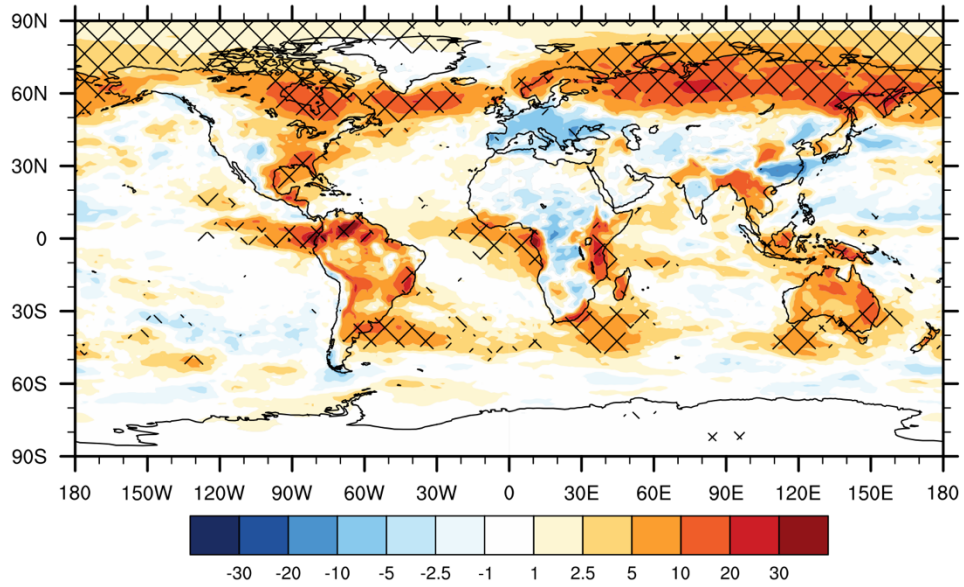

Figure R3 Fire aerosol induced low-level cloud fraction change (unit: %) in the CESM-RESFire present-day simulation (CTRL1-SENS1A).

Page 8, Line 279: It would be good to briefly introduce this plume rise parameterization (e.g., based on what measurements? Global universal or regional-based?)
Response: Thank you for the suggestion. The Sofiev et al. (2012) plume rise parameterization is globally universal and is based on atmospheric boundary layer height, fire radiative power, and Brunt-Väisälä frequency in the free troposphere. We added relevant description in line 299-302 as follows:
"In our simulations, we used a simplified plume rise parameterization (Sofiev et al., 2012) based on online calculated fire burning intensity (FRP) and atmospheric stability conditions (PBLH and Brunt-Väisälä frequency) in CESM-RESFire and applied vertical profiles with diurnal cycles to the vertical distribution of fire emissions".

Page 11, Line 376-379: The terms 'fire combustion factors', 'fire spread distribution', and 'fire spread factors' are probably not familiar to many readers. Please consider a short explanation on these parameters (i.e., what do they mean physically).
Response: Thanks. Fire combustion factors (FCF) are based on 10-day running mean of surface temperature, 10-day running mean of total precipitation, and soil water fraction for top 0.05 m layers as a surrogate for fuel combustibility (see Table 3 of Zou et al. (2019)), while fire spread factors (FSF) include surface air temperature, relative humidity, surface soil wetness, and fractions of wet canopy as listed in Table 4 of Zou et al. (2019). We added the explanation for these terms in line 396-397 and line 400-401 of the revised manuscript.

Page 11, Line 388-389: I don't quite understand the causal relationship stated in this sentence. The changes in wind speed are higher over the ocean than that over land, but this could be

simply due to the larger magnitude of wind speed over the ocean. Relatively smaller changes in land wind speed could still have large impacts on fire spread and burned area.
Response: Thank you for the comment. We rewrote the analysis for climate-fire-ecosystem interactions in Sect. 3.3. Please see the revised manuscript for details.

Page 25, Figure 2: Please align tick label '0.1' with other tick labels in panels b, c, d.
Response: Thanks. The figure has been updated.

Page 27, Line 817: Should the unit of CDNUMC '10^9 # /m2' (as correctly shown in panel d)?
Response: That's correct. Thanks for the correction.

Page 30, Figure 7: The colors in panel c don't have enough separation. Please use another scale.
Response: Thank you. The scale in this figure has been updated for better color separation.

Page 32, Figure 9: If my understanding is correct, the data in this figure show the differences of fire modifications on weather variables between the future and present ((CTRL2-SENS2B)-(CTRL1-SENS1B)), not the differences of weather variables (in CTRL model) between the future and present (CTRL2-CTRL1). The current form of figure caption is a bit confusing.
Response: Thank you for the correction. Fig. 9 is used to explain the future changes in simulated global fire activity. Therefore, we compare the future and present-day fire weather conditions in CTRL2 and CTRL1 to understand these fire simulation results shown in Figs. 7 and 8. This figure has been updated with the corresponding sensitivities to surface temperature, precipitation, relative humidity, and surface wind speed between CTRL2 and CTRL1. The changes in fire feedback on these fire weather variables (i.e., (CTRL2-SENS2B)-(CTRL1-SENS1B)) are shown in Fig. 10 with corresponding discussion in Sect. 3.3 of the revised main text.

References

Andela, N., Morton, D. C., Giglio, L., Chen, Y., van der Werf, G. R., Kasibhatla, P. S., DeFries, R. S., Collatz, G. J., Hantson, S., Kloster, S., Bachelet, D., Forrest, M., Lasslop, G., Li, F., Mangeon, S., Melton, J. R., Yue, C., Randerson, J. T.: A human-driven decline in global burned area, Science, 356(6345), 1356–1362. https://doi.org/10.1126/science.aal4108, 2017.

Andela, N., and van der Werf, G. R.: Recent trends in African fires driven by cropland expansion and El Nino to La Nina transition, Nature Climate Change, 4, 791–795. https://doi.org/10.1038/nclimate2313, 2014.

Clark, S. K., Ward, D. S., and Mahowald, N. M.: Parameterization-based uncertainty in future lightning flash density, Geophys. Res. Lett., 44, 2893–2901, doi:10.1002/2017GL073017, 2017.

Sofiev, M., Ermakova, T., and Vankevich, R.: Evaluation of the smoke-injection height from wild-land fires using remote-sensing data, Atmos. Chem. Phys., 12, 1995-2006, 10.5194/acp-12-1995-2012, 2012.

Tost, H., Jöckel, P., and Lelieveld, J.: Lightning and convection parameterisations – uncertainties in global modelling, Atmos. Chem. Phys., 7, 4553–4568, https://doi.org/10.5194/acp-7-4553-2007, 2007.

Zou, Y., Wang, Y., Ke, Z., Tian, H., Yang, J., and Liu, Y.: Development of a REgion-Specific ecosystem feedback Fire (RESFire) model in the Community Earth System Model, J. Adv. Model Earth Sy., https://doi.org/10.1029/2018MS001368, 2019.

Responses to referee #2:

The manuscript by Zou et al. presents an analysis of the interactions between climate, wildfires, ecosystems, and radiative balance in a recently (further) developed modelling system, CESM-RESFire. The methodology includes a suitable set of sensitivity experiments that provide substantial new insight into the role of different types of potential interactions (mainly aerosol effects and land cover changes) in driving present-day radiative effects of wildfires, and their future radiative forcing. It features some novel aspects compared to previous studies, especially when it comes to the types of feedbacks allowed and investigated, and provides a useful contribution to the improvement of our poor understanding of the role of fire in the Earth system. The manuscript is nicely written, and well within the scope of Atmospheric Chemistry and Physics. I find it worthy of publication, following some (mostly minor) improvements that I describe below.

Response: Thank you for your constructive comments and helpful suggestions. We revised the manuscript following the suggested improvements. Please see below the point-by-point responses with corresponding revisions in the manuscript.

GENERAL COMMENTS:

- The title, abstract and conclusions (as well as the main text) leave the reader thinking that the full climate effects of wildfires are examined in the current study. However, this is somewhat misleading, as full climate responses (i.e. temperature, precipitation, humidity etc changes) are not explored or discussed, even if they are partially included (I am saying "partially" since the oceans and sea-ice are fixed). The study goes up to radiative effect and radiative forcing quantification, and that should be reflected more accurately in the different parts of the text. In my specific comments below, there are some suggestions for amending this, but the authors should make an effort to do so further throughout the text.

Response: Thank you for the suggestion. We added two new figures (Fig. 9 and 10) and relevant discussion in Sect. 3.3 of the main text to examine future changes in full climate responses (Fig.9: CTRL2-CTRL1) of fire weather variables (surface air temperature, precipitation, relative humidity, and surface wind speed) as well as these associated with fire feedbacks (Fig. 10: (CTRL2-SENS2B)-(CTRL1-SENS1B)) to explore fire-climate interactions. The fire weather changes without fire feedbacks (SENS2B-SENS1B) are shown in Fig. S3 in the supplement for comparison. Please see our responses to your specific comments below for more details.

- In addition, the future radiative impacts (whose study presumably is a core aim of this work) are discussed very briefly towards the end of Sect. 3.3, and in a way that does not seem accurate/consistent with what is shown on the maps (see related comment below).

Response: Thank you. We rewrote the major part in Sect. 3.3 with more detailed and consistent discussion for climate-fire-ecosystem interactions and fire radiative forcing. Please see Sect. 3.3 in the revised manuscript for details.

- The past tense is often used in the text to refer to the work presented here, where the present tense would be more appropriate/standard. For example "We provided a brief model description and sensitivity experiment settings in Section 2. . .", where "provide" would probably read better. I suggest making this amendment to wherever applicable in the text.

Response: Thank you. We made the amendments with proper tense throughout the manuscript as suggested for better presentation.

SPECIFIC COMMENTS:
Page 2, Lines 1-3: I suggest changing the title to "Using CESM-RESFire to Understand Climate-Fire-Ecosystem Interactions and their Implications for Radiative Forcing". The title as it stands currently is misleading, as "implications for decadal climate variability" were not examined at all in this study. Generally speaking, it is radiative forcing/effects that were examined, rather than climate (temperature, humidity, precipitation etc) effects.
Response: Thank you for the suggestion. In our response to the above general comments, we added two new figures (Fig. 9 and 10) in the main text and one more figure (Fig. S3) in the supplement to fully evaluate fire weather and climate responses to different driving factors such as increased GHG concentrations and fire feedback through multiple pathways. Besides, we also discussed the carbon budget response to fire disturbances in the present-day and future scenarios in Sect. 3.2, which is one of the major research objectives for the comprehensive evaluation of climate-fire-ecosystem interactions and future projections in this work. Radiative forcing and carbon budget were used as two evaluation metrics for these objectives. Therefore, we partially accepted your suggestion and changed the title to "Using CESM-RESFire to Understand Climate-Fire-Ecosystem Interactions and the Implications for Decadal Climate Variability".

Page 1, Line 20: For the same reason, I suggest rephrasing to ". . .and their impacts on fire activity and radiative forcing".
Response: Thank you for the suggestion. We discussed fire impacts on carbon budget in Sect. 3.2. We also added more figures and discussion in Sect. 3.3 of the revised manuscript to improve our analysis on fire feedbacks to the climate systems and fire activity itself.

Page 2, Line 38: Please add ", respectively" at the end of the sentence.
Response: Thank you. It's added.

Page 2, Lines 57-58: "are further confounded by natural processes and human interferences" – human and natural processes have been mentioned in the previous sentence. Why repeat them?
Response: Thank you. We removed this sentence as suggested.

Page 2, Line 69: "used the same approach" – suggest changing to "used the same unidirectional approach".
Response: Thank you. We added "unidirectional" in this sentence as suggested.

Page 2, Line 71: The term "fixed" may not be fully accurate here. For example, to my knowledge, Tosca et al. (2013) performed simulations with and without aerosol emissions, with no "fixing" per se involved.
Response: Thank you. Tosca et al. (2013) used monthly cycling
1997–2009 fire emissions based on the GFEDv3 dataset. Therefore, we changed "fixed" here to "prescribed".

Page 3, Line 79: I do not think "feedback in" is needed.
Response: Thank you. It's removed.

Page 3, Lines 81-84: Change past tense to present tense (just another example).
Response: Thank you. We changed past tense to present tense wherever applicable in the manuscript.

Sect. 2.1: Gas-phase chemistry (e.g. ozone and its precursors) is not mentioned at all in the model description – or anywhere really. If such a mechanism is not included, this should be mentioned (along with acknowledging the potentially sizeable effect of this missing process), and if included, the authors should describe in what fashion it is included.
Response: Thank you. We used a no gas-phase chemistry version of the CAM5 model with prescribed O_3 concentrations. Therefore, we didn't consider photochemical reactions and chemistry-climate feedbacks in our discussion. We added an explanation in line 102-103 as follows: "The gas-phase photochemistry is not included in the CAM5 simulations, which precludes the possibility for evaluating chemistry-climate interactions".

Sect. 2.1: No mention at all of biogenic aerosols.
Response: In CAM5, biogenic emissions of volatile organic compounds (isoprene, monoterpenes, toluene, big alkenes, and big alkanes) are pre-defined and read from an input emission file derived from MOZART VOC emissions. Then a simple treatment of secondary organic aerosol (SOA) is used to assume fixed mass yields (Table R1) for anthropogenic and biogenic precursor VOCs (Neale et al., 2013). The total yielded mass is emitted as the SOA (gas) species and condensation/evaporation of the SOA (gas) to/from three aerosol modes are calculated in the MAM3 module.

We added the description of biogenic aerosols in CAM5 in line 98-102 of this section: "A simple treatment of secondary organic aerosols (SOA) is used in CAM5 to derive SOA formation from anthropogenic and biogenic volatile organic compounds (VOCs) with fixed mass fields (Table S1 in the Supplement). The total SOA mass is emitted as the SOA (gas) species from the surface and then condensation/evaporation of gas-phase SOA to/from different aerosol modes are calculated in the MAM3 module (Neale et al., 2013)", and the information of input files in line 142-144 of Sect. 2.2: "Emission fluxes for the 5 VOC species (isoprene, monoterpenes, toluene, big alkenes, and big alkanes) to derive SOA mass yields were prescribed from the MOZART-2 dataset (Horowitz et al., 2003)".
We also added a new table (Table S1) of SOA (gas) mass yields in the supplement.

Table R1 Assumed SOA (gas) yield in CAM5

Species	Mass yield	Reference
Big Alkanes	5%	Lim and Ziemann (2005)
Big Alkenes	5%	Assumed
Toluene	15%	Odum et al. (1997)
Isoprene	4%	Kroll et al. (2006)
Monoterpenes	25%	Ng et al. (2007)

Page 3, Line 97: Probably "microphysics" and not "macrophysics"?

Response: The parameterization of stratiform cloud microphysics is based on Morrison and Gettlman (2008). Its implementation in the CAM model is described in Gettelman et al. (2008). Cloud macrophysics is suite of physical processes that computes (1) cloud fractions in each layer; (2) horizontal and vertical overlapping structures of clouds; (3) net conversion rates of water vapor into cloud condensates. Its parameterization and implementation in CAM5 are described in Park et al., 2014.

We added the cloud microphysics scheme in line 97-98 of the revised manuscript. Please refer to Sect. 4.6 "Cloud Microphysics" and Sect. 4.7 "Cloud Macrophysics" of the CAM5 Tech Notes (Neale et al., 2013) for more details.

Page 4, Line 110: Please mention the year for the future scenario. It's mentioned later, but worth mentioning it here too.
Response: Thank you. We added the modeling years for both scenarios here.

Page 4, Lines 138-140: Suggested rephrasing – ". . .we allowed the semi-static historical LCC data for the year 2000 from the version 1 of the Land-Use History A product (LUHa.v1) (Hurtt et al., 2006) to be affected by post-fire vegetation changes (Zou et al., 2019)".
Response: Thank you. We revised the sentence as suggested.

Page 5, Lines 150-151: "given great uncertainties in future projections of these inputs" - Are these uncertainties larger than for the rest of the variables considered here?
Response: Lightning is critical for atmospheric chemistry and wildfire simulations. Its parameterizations in global models differ greatly among the models and have very large uncertainties. Several studies have compared different lightning parameterizations and evaluated the uncertainties in future projections. For instance, Tost et al. (2007) compared different combinations of convection and lightning parameterizations with satellite observations and found a wide range in the spatial and temporal variability of the simulated lightning flash density. Similarly, Clark et al. (2017) evaluated the performance of 8 lightning parameterizations in CAM5 and tested the sensitivity of future lightning activity to the choice of parameterization. They found that future changes in global mean lightning flash density are highly sensitive to the parameterization chosen, with cloud top height schemes, a cold cloud depth scheme, and a scheme based on convective mass flux projecting large increases (36% to 45%), a mild increase (12.6%), and a decrease (−6.7%) in lightning flash density, respectively, under the RCP8.5 scenario. Finney et al. (2018) got a similar conclusion by comparing a new upward cloud ice flux (IFLUX) approach with the widely used cloud-top height (CTH) approach, with a 15% decrease in total lightning flash rate in 2100 under RCP8.5 based on IFLUX in contrast to previously reported global increase in lightning based on CTH. They also identified the largest differences in the tropics where most lightning and fires occur.

Moreover, these regions are also heavily affected by anthropogenic activities such as deforestation and agriculture expansion (Andela et al., 2017;Morton et al., 2008;Van der Werf et al., 2010). The future changes in human activities and associated land use and land cover change are also strongly dependent on the choice of different socioeconomic development pathways (Riahi et al., 2017).

In this work, we decided to use observation-based lightning and present-day demographic data in our fire simulations in order to focus on climate-fire-ecosystem interactions that are of interest of this study. We revised the discussion in line 159-164 to "It is worth noting that we used the present-day demographic data and observation-based climatological lightning data in the future scenario given pathway-dependence and great uncertainties in future projections of these inputs (Clark et al., 2017;Riahi et al., 2017;Tost et al., 2007;). In other words, we did not consider the influence of fire ignition changes associated with human activity or lightning flash density in our future projection simulations but focused on broad impacts of future climate change on fuel loads and combustibility as well as fire weather conditions", and added a new section 3.4 to discuss the relevant uncertainties.

Page 5, Lines 161-164: Yes, but are the timescales long enough in this case for this assumption to hold? Please discuss.

Response: In our fire model development study (Zou et al., 2019), we evaluated the post-fire temporal evolution of carbon budget variables in different regions. Here we reproduced Fig. S3 in Zou et al. (2019) to show these changes in an idealized burning experiment, in which we conducted single-year burning events in fire peak months of 7 typical fire-prone regions. The post-fire recovery rates in net ecosystem productivity (NEP, g C m^{-2} yr^{-1}, positive for net ecosystem carbon uptake) vary among different PFT groups with the mean recovery periods of post-fire NEP about 3–18 years. For most regions, the recovery time is less than or about the simulation time period in this study. Therefore, we consider this assumption valid in general. Since ocean and terrestrial carbon sinks are not simulated in this study, we had to rely on a "concentration-driven" approach instead of the "emission-driven" one by prescribing atmospheric CO_2 concentrations in each modeling scenario. A series of comprehensive assessments of the global carbon cycle are available by using observation-constrained modeling estimates of all carbon sources and sinks (Le Quéré et al., 2018a; Le Quéré et al., 2018b), which is out of the scope of this study.

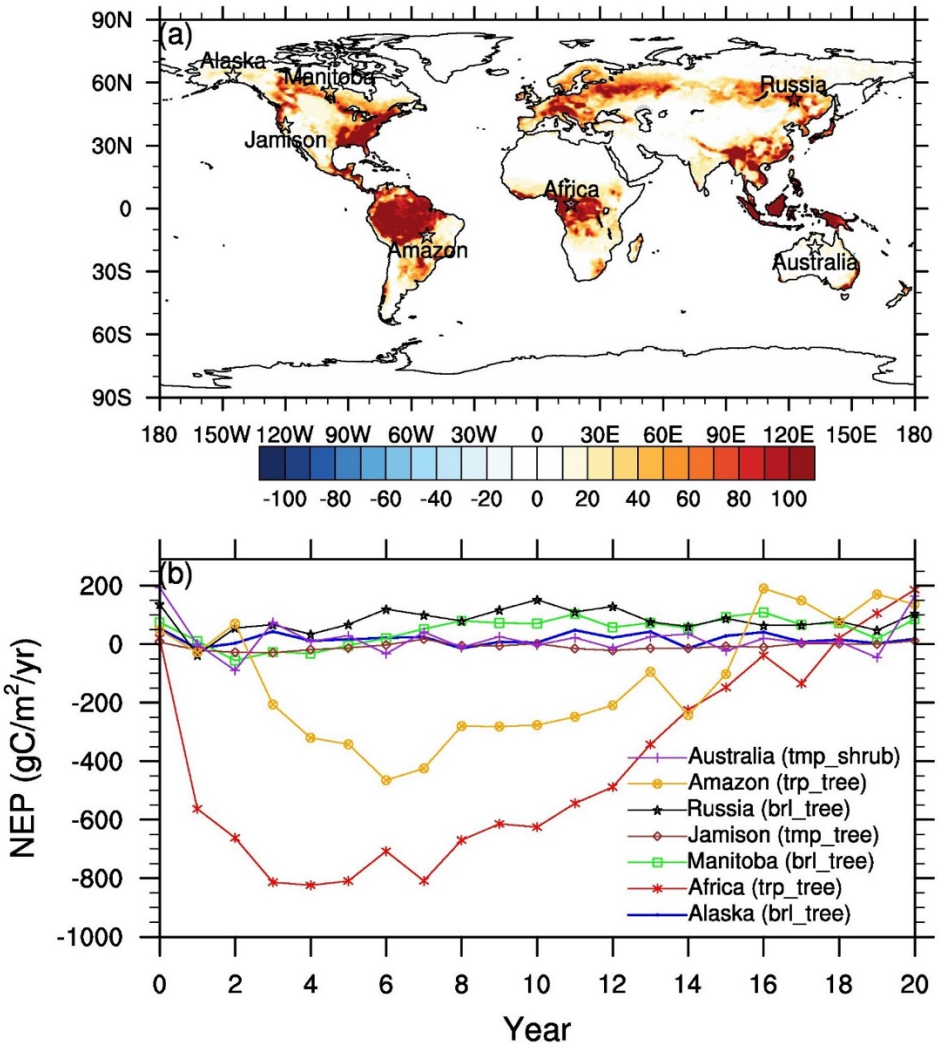

Figure R1. Simulated post-fire temporal evolution of carbon budget in different PFT regions based on an idealized burning experiment. (a) spatial distributions of annual averaged NEP (gC m^{-2} yr^{-1}); (b) temporal variations of post-fire NEP in each disturbed mode grid cell. tmp_shrub: temperate shrub dominated; trp_tree: tropical forest dominated; brl_tree: boreal forest dominated; tmp_tree: temperate forest dominated. (reproduced from Fig. S3 in Zou et al., 2019)

Page 5, Line 175: "the Ghan's method" -> "the Ghan method"
Response: Thank you. It is changed as suggested.

Equations (1): The way these equations are written is very confusing. First of all because of the dashes ("-") and the minuses appearing identical, and also because of the use of column (:). I suggest the following format:
"RE of interaction of radiation with fire aerosol: RE = Δ(F -F)" (with the appropriate subscripts in each case)
Response: Thank you. We revised the equations as suggested.

Page 6, Line 188: "nonnegligible" -> "non-negligible"
Response: Corrected. Thanks.

Page 6, Line 200: “budge” -> “budget”
Response: Corrected. Thanks.

Page 7, Lines 220-221: “However, the model well captured the high AOD regions over the Northern and Southern Hemispheres of Africa” – I am not sure I see this on Fig. 1. Therefore the statement seems too confidently positive.
Response: Thank you for the comment. We revised the description in line 232-235 to “The AOD simulations over tropical savanna regions with pervasive biomass burning activities are also lower than the satellite observations, which might be attributable to both underestimated online fire emissions and too strong wet scavenging of primary carbonaceous aerosols in the CAM5-MAM3 model (Liu et al., 2012)”.

Page 7, Line 228: The AERONET measurements cannot be characterised as “in situ”. They are also remotely sensed.
Response: Corrected. Thanks.

Fig. 3: Please specify that this is TOA radiative effect.
Response: The description was added in the figure caption. Thanks.

Page 7, Lines 243-247: There are some areas that experience pronounced positive forcing due to fire aerosol-cloud interactions. The most prominent ones are Europe and most of Africa. Presumably that is because of black carbon stabilization effects? But why would these be more important in these specific regions? Any thoughts? Please comment.
Response: Fig. R2 shows the changes in low-level cloud fractions induced by fire aerosols in the present-day simulation (CTRL1-SENS1A). It demonstrates decreased low-level clouds over Europe and most of African land regions and increased clouds over most of the other regions. Therefore, positive radiative forcing is found over these land regions concurrent with reduced cloud coverage in contrast to other regions with increased cloud coverage (Fig. 3b in the manuscript). Though these decreased clouds are not statistically significant, the cooling of the surface due to fire aerosol scattering stabilizes the lower atmosphere and reduces cloud formation. We added Fig. S1 in the supplement and added more detailed explanation in line 261-265 as follows:
“The large amounts of fire aerosols suppress low-level clouds over the African land region by stabilizing the lower atmosphere through reduction of radiative heating of the surface. However, fire aerosols increase cloud cover and brightness in the downwind Atlantic Ocean areas because they increase the number of cloud condensation nuclei and the larger cloud droplet number density reduce cloud droplet sizes (Lu et al., 2018; Rosenfeld et al., 2019; Fig. S1 in the Supplement)”.

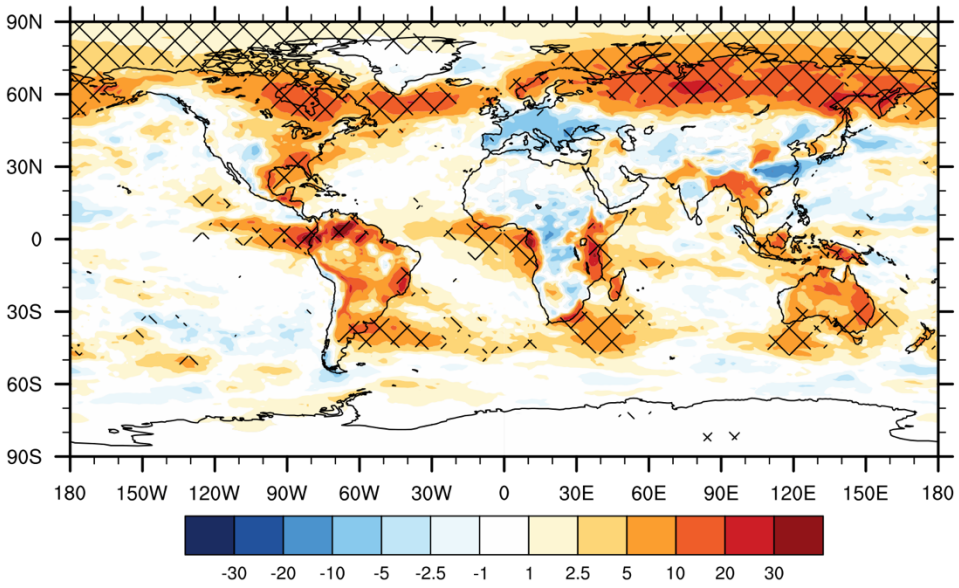

Figure R2 Fire aerosol induced low-level cloud fraction change (unit: %) in the CESM-RESFire present-day simulation (CTRL1-SENS1A). The net meshes denote the 0.05 significance level.

Page 8, Lines 248-249: Why are there areas with both positive and negative changes? Why is Africa pretty much all negative? These are interesting features. Please elaborate.

Response: The estimate of the radiative effect associated with fire aerosol-induced surface albedo change is based on the Ghan method (2013), which considers both changes in snow albedo due to deposition of light-absorbing fire aerosol, and changes in snow cover induced by fire aerosol caused precipitation change. As shown by Fig. R3a, the snow depths decrease in most Arctic regions in CTRL1, suggesting snow albedo reduction due to deposition of absorptive aerosols to snow. In contrast, these regions in Canada, eastern Siberia, and Tibet show increased surface albedo in Fig. R3b, which results from increases in snowfall and snow cover over these regions. These surface albedo changes modulate the reflection of incoming solar radiation and finally alter the net shortwave radiative flux at the TOA (Fig. 3c in the manuscript). The fire aerosol-induced albedo effect is more significant in high-latitude regions than others because of the spatial distribution of snow cover and snow precipitation. Other factors like numerical noise might also contribute to these simulated radiation changes between the two experiments.

We added the above discussion in line 265-270 and Fig. S2 in the supplement.

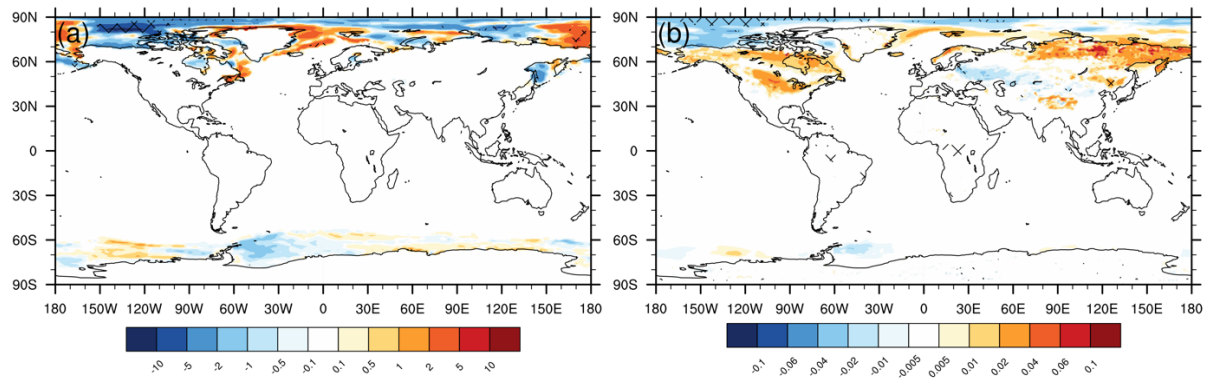

Figure R3 Fire aerosol induced snow and albedo changes between CTRL1 and SENS1A. (a) changes in snow depths (m) over ice; (b) changes in surface albedo (unitless). The net meshes denote the 0.05 significance level.

Page 8, Lines 262-263: Please specify that the Jiang et al. (2016) study was performed with the same atmospheric model as in the current study (though older version?), as it is useful for the reader to know.
Response: Thank you. Jiang et al. (2016) used the same version of the CAM5 model (CAM5 version 5.3) but with a 4-mode modal aerosol module (MAM4). We added this information in line 282-284.

Page 9, Line
293: I am not sure where the +51% value comes from. From Table 2, the Raci is -1.31 for 2050 in this study and -1.42 in the CCSM study. Or do the authors mean something different and I am missing the point? In any case, I think it should be made clearer where the +51% value comes from.
Response: Here the percentage indicates the change in net fire radiative forcing estimated by Ward et al. (2012), which increases by 51% from -0.55 W/m^2 in the 2000s to -0.83 W/m^2 in the 2100s based on the CCSM forcing data. We revised the discussion in line 471-473 to "This projection result is larger than the change in net fire radiative forcing based on the CCSM future projection in Ward et al. (2012), which suggested a 51% increase from -0.55 W m^{-2} in the 2000s to -0.83 W m^{-2} in the 2100s (Table 2)".

Page 9, Lines 313-315: "Such difference is also consistent with the changes in different versions of the GFED datasets, which show a 11% increase of global fire carbon emissions in the latest GFED4s as compared with the old GFED3 for the overlapping 1997-2011 time period (van der Werf et al., 2017)" – Do the authors mean that there is an upward "trend" between older and newer GFED emissions versions, implying that eventually the GFED emissions will match the online model? That's a rather simplistic reasoning and needs to be supported further or phrased differently.
Response: The difference of fire carbon emissions between the new GFED4s data and the old GFED3 data is a result of estimation changes in both global burned area and mean fuel consumption (van der Werf et al., 2017). The GFED4s data includes burned area and emission estimates from small fires that are missing in the old GFED3 data. These small fires were difficult to be resolved by satellite remote sensing techniques before. The new dataset used a revised version of the Randerson et al. (2012) small-fire estimation approach to include these small fires. We added the explanation in line 331-333 as "This increased global fire carbon emissions in the GFED4s dataset result from a substantial increase in global burned area (+37%) due to inclusion of small fires and a modest decrease in mean fuel consumption (-19%) according to van der Werf et al. (2017)".

Page 11, Lines 361-363: "Though we mainly focused on fire-climate interactions without consideration of human impacts in this study, the RESFire model is capable of reproducing the anthropogenic interference on fire activity as observed from the space (Zou et al., 2019)" – This needs some more explanation. The common understanding is that in Northern Hemisphere Africa the decline in burned area is due to agricultural conversion and resulting landscape fragmentation (e.g. Andela et al., 2017). Is this a process that is represented in this particular model? Please clarify and discuss.

Response: Before using the RESFire model for future projections, we comprehensively evaluated its modeling performance in terms of both spatial distributions and temporal variations for global burned area and fire emissions in our previously published model development paper (Zou et al., 2019). The RESFire model is capable to reproduce the observed decadal trends driven by different forcing factors such as decadal climate variability as well as demographic and socioeconomic changes (as shown in Fig. R3 and in Andela and van der Werf, 2014 and Andela et al., 2017). However, since climate-fire-ecosystem interactions are of interest in this work, we fixed socioeconomic factors such as population density and GDP in the RESFire simulations and projections. We added more explanation and discussion in line 379-382 as follows:
"Though we mainly focus on fire-climate interactions without consideration of human impacts in this study, the RESFire model is capable of capturing the anthropogenic interference on fire activity and reproducing observation-based long-term trends of regional burning activity driven by climate change and human factors (Zou et al., 2019)".

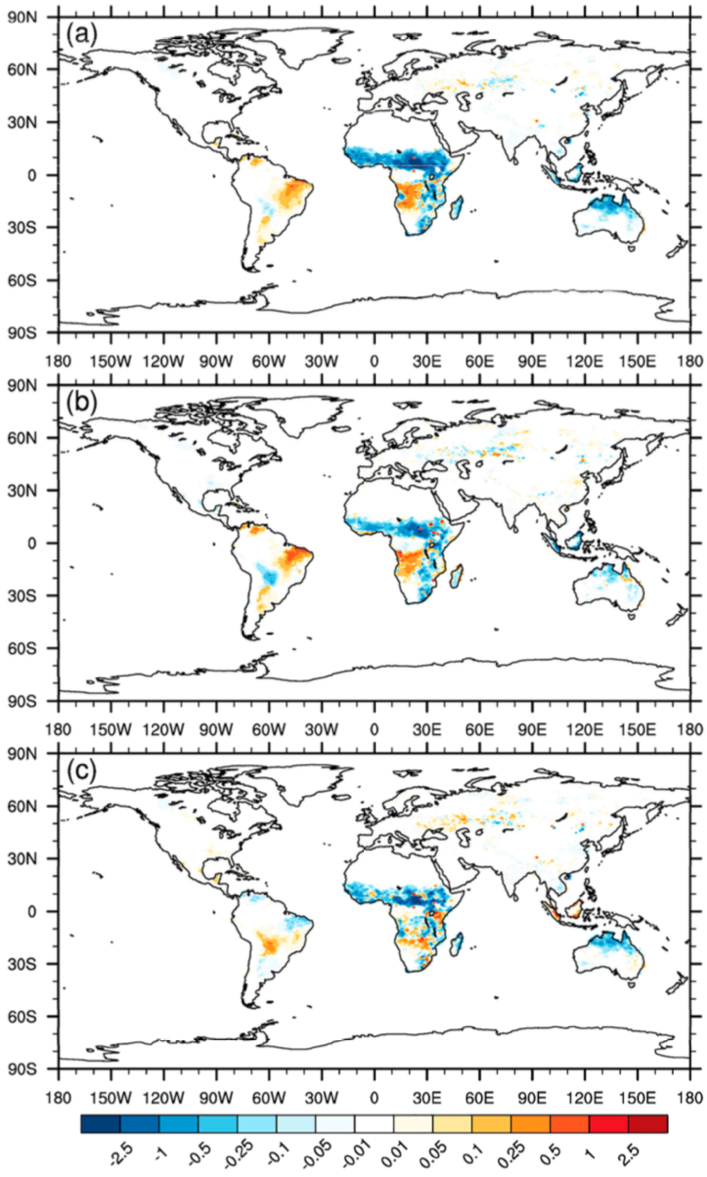

Figure R4 Comparisons of decadal trends (%/year) in annual averaged burned areas from 1991 to 2010. (a) Burned area trends driven by natural and demographic forcing in RESFire_CRUNCEPa with changing weather and population; (b) burned area trends driven by only natural forcing in RESFire_CRUNCEPb with changing weather but fixed population density; (c) burned area trends driven by demographic changes only. RESFire = REgion- Specific ecosystem feedback Fire; CRUNCEP = Climatic Research Unit and National Centers for Environmental Prediction. (reproduced from Fig. 10 in Zou et al., 2019)

Page 11, Lines 390-394: The evidence to support this statement is somewhat weak. First of all, the precipitation changes (Fig. 9c) are not significant almost everywhere (therefore, not much difference in that respect to the wind changes). Secondly, the match between locations with decreased precipitation and increased burned area (and the other way around) is not always clear (e.g. the north of Siberia experiences increases in burned area, but simultaneous increases in precipitation; there are other examples too). It would be best to discuss this in a more quantitative fashion, e.g. report the spatial correlation coefficients between burned area and driver variables to extract more robust conclusions?
Response: Thank you for the suggestion. We added the spatial correlation coefficients in line 403-404. We also rewrote the major part of Sect. 3.3 with more detailed discussion of climate-fire-ecosystem interactions. Please see the revised manuscript for details.

Figure 11: This figure is not really discussed in any insightful way, beyond just stating that such effects "might compensate biogeochemical warming effects of deforestation related carbon-cycle changes". How does each individual variable shown affect warming/cooling patterns, and which of these variables seems to be more important, based on this analysis?
Response: The fire related albedo change and radiative effect are not as significant as suggested by previous studies. Therefore, we moved this figure from the main text to the supplement (Fig. S6) in the revised manuscript and added corresponding discussion in line 461-465 as follows: "Previous studies have suggested a net cooling effect of deforestation that could compensate for GHG waring effects on a global scale (Bala et al., 2007;Jin et al., 2012;Randerson et al., 2006). Though our model captures the reduction of forest coverage and increased springtime albedo in high-latitude regions (Fig. S6 in the Supplement), the radiative effect of fire induced LCC is almost neutral on a global basis in both present-day and future scenarios (Table 2)".

Page 12, Lines 427-431: This discussion is rushed and I am not sure I follow the reasoning. It is stated that the radiative forcing of aerosol-radiation interactions "show similar patterns with Fig. 3a, with generally cooling effects over the vicinities of fire areas and warming effects over the downwind regions". Where do we see this? In Fig. 3a, this was evident e.g. in and around Africa (and possibly South America), but I cannot see this in Fig. 12c. Then for aerosol-cloud interactions, it is stated that there are "warming effects in Southeast Asia and Australia due to local cloud changes", but how are these features consistent with Fig. 3b, in which the inclusion of fire caused negative radiative effects due to aerosol-cloud interactions over those regions (as was the case for northern high latitudes).
Response: We rewrote the major part of Sect. 3.3 with more detailed and consistent discussion of climate-fire-ecosystem interactions. Please see the revised manuscript for details.

Page 13, Line 447: Please add "fire" between "significant" and "aerosol".
Response: The cooling effect is mainly contributed by aerosols from anthropogenic and industrial emission sources in the eastern U.S. and China. Therefore, we prefer to keep it as is to be consistent with the references cited here.

Page 13, Lines 455-456: Please change “climate effects” to “radiative effects”, as the former implies that effects on temperature, precipitation etc due to fires were also examined (which is not the case).
Response: We discussed fire feedback effects on climate and weather variables such as air temperature, precipitation, relative humidity, and surface wind speed in Fig. 10 and line 419-428 of the revised manuscript. Please see Sect. 3.3 for more details.

Page 13, Line 465: Please change “their” to “its”.
Response: Thanks. This sentence is changed to “More evaluation metrics such as large wildfire extreme events should be considered in future studies to improve our understanding of global and regional fire activities, their variations and trends, and their relationship with decadal climate change.”.

References

Andela, N., and van der Werf, G. R.: Recent trends in African fires driven by cropland expansion and El Nino to La Nina transition, Nature Climate Change, 4, 791–795. https://doi.org/10.1038/nclimate2313, 2014.

Andela, N., Morton, D.C., Giglio, L., Chen, Y., Van Der Werf, G.R., Kasibhatla, P.S., DeFries, R.S., Collatz, G.J., Hantson, S., Kloster, S. and Bachelet, D.: A human-driven decline in global burned area. Science, 356(6345), 1356-1362, 2017.

Clark, S.K., Ward, D.S. and Mahowald, N.M.: Parameterization-based uncertainty in future lightning flash density. Geophysical Research Letters, 44(6), 2893-2901, 2017.

Finney, D.L., Doherty, R.M., Wild, O., Stevenson, D.S., MacKenzie, I.A. and Blyth, A.M.: A projected decrease in lightning under climate change. Nature Climate Change, 8(3), 210, 2018.

Ghan, S. J.: Technical Note: Estimating aerosol effects on cloud radiative forcing, Atmos. Chem. Phys., 13, 9971–9974, https://doi.org/10.5194/acp-13-9971-2013, 2013.

Gettelman, A., Morrison, H. and Ghan, S.J.: A new two-moment bulk stratiform cloud microphysics scheme in the Community Atmosphere Model, version 3 (CAM3). Part II: Single-column and global results. Journal of Climate, 21(15), 3660-3679, 2008.

Kroll, J.H., Ng, N.L., Murphy, S.M., Flagan, R.C. and Seinfeld, J.H.: Secondary organic aerosol formation from isoprene photooxidation. Environmental science & technology, 40(6), 1869-1877, 2006.

Le Quéré, C., Andrew, R. M., Friedlingstein, P., Sitch, S., Pongratz, J., Manning, A. C., Korsbakken, J. I., Peters, G. P., Canadell, J. G., Jackson, R. B., Boden, T. A., Tans, P. P., Andrews, O. D., Arora, V. K., Bakker, D. C. E., Barbero, L., Becker, M., Betts, R. A., Bopp, L., Chevallier, F., Chini, L. P., Ciais, P., Cosca, C. E., Cross, J., Currie, K., Gasser, T., Harris, I., Hauck, J., Haverd, V., Houghton, R. A., Hunt, C. W., Hurtt, G., Ilyina, T., Jain, A. K., Kato, E., Kautz, M., Keeling, R. F., Klein Goldewijk, K., Körtzinger, A., Landschützer, P., Lefèvre, N., Lenton, A., Lienert, S., Lima, I., Lombardozzi, D., Metzl, N., Millero, F., Monteiro, P. M. S., Munro, D. R., Nabel, J. E. M. S., Nakaoka, S., Nojiri, Y., Padin, X. A.,

Peregon, A., Pfeil, B., Pierrot, D., Poulter, B., Rehder, G., Reimer, J., Rödenbeck, C., Schwinger, J., Séférian, R., Skjelvan, I., Stocker, B. D., Tian, H., Tilbrook, B., Tubiello, F. N., van der Laan-Luijkx, I. T., van der Werf, G. R., van Heuven, S., Viovy, N., Vuichard, N., Walker, A. P., Watson, A. J., Wiltshire, A. J., Zaehle, S., and Zhu, D.: Global Carbon Budget 2017, Earth Syst. Sci. Data, 10, 405–448, https://doi.org/10.5194/essd-10-405-2018, 2018a.

Le Quéré, C., Andrew, R. M., Friedlingstein, P., Sitch, S., Hauck, J., Pongratz, J., Pickers, P. A., Korsbakken, J. I., Peters, G. P., Canadell, J. G., Arneth, A., Arora, V. K., Barbero, L., Bastos, A., Bopp, L., Chevallier, F., Chini, L. P., Ciais, P., Doney, S. C., Gkritzalis, T., Goll, D. S., Harris, I., Haverd, V., Hoffman, F. M., Hoppema, M., Houghton, R. A., Hurtt, G., Ilyina, T., Jain, A. K., Johannessen, T., Jones, C. D., Kato, E., Keeling, R. F., Goldewijk, K. K., Landschützer, P., Lefèvre, N., Lienert, S., Liu, Z., Lombardozzi, D., Metzl, N., Munro, D. R., Nabel, J. E. M. S., Nakaoka, S., Neill, C., Olsen, A., Ono, T., Patra, P., Peregon, A., Peters, W., Peylin, P., Pfeil, B., Pierrot, D., Poulter, B., Rehder, G., Resplandy, L., Robertson, E., Rocher, M., Rödenbeck, C., Schuster, U., Schwinger, J., Séférian, R., Skjelvan, I., Steinhoff, T., Sutton, A., Tans, P. P., Tian, H., Tilbrook, B., Tubiello, F. N., van der Laan-Luijkx, I. T., van der Werf, G. R., Viovy, N., Walker, A. P., Wiltshire, A. J., Wright, R., Zaehle, S., and Zheng, B.: Global Carbon Budget 2018, Earth Syst. Sci. Data, 10, 2141–2194, https://doi.org/10.5194/essd-10-2141-2018, 2018b.

Lim, Y.B. and Ziemann, P.J.: Products and mechanism of secondary organic aerosol formation from reactions of n-alkanes with OH radicals in the presence of NOx. Environmental science & technology, 39(23), 9229-9236, 2005.

Morton, D.C., Defries, R.S., Randerson, J.T., Giglio, L., Schroeder, W. and Van Der Werf, G.R.: Agricultural intensification increases deforestation fire activity in Amazonia. Global Change Biology, 14(10), 2262-2275, 2008.

Morrison, H. and Gettelman, A.: A new two-moment bulk stratiform cloud microphysics scheme in the Community Atmosphere Model, version 3 (CAM3). Part I: Description and numerical tests. Journal of Climate, 21(15), 3642-3659, 2008.

Neale, R. B., Chen, C. C., Gettelman, A., Lauritzen, P. H., Park, S., Williamson, D. L., Conley, A. J., Garcia, R., Kinnison, D., Lamarque, J. F., Marsh, D., Mills, M., Smith, A. K., Tilmes, S., Vitt, F., Morrison, H., Cameron-Smith, P., Collins, W. D., Iacono, M. J., Easter, R. C., Ghan, S. J., Liu, X. H., Rasch, P. J., and Taylor, M. A.: Description of the NCAR Community Atmosphere Model (CAM 5.0), NCAR 289, 2013.

Ng, N.L., Chhabra, P.S., Chan, A.W.H., Surratt, J.D., Kroll, J.H., Kwan, A.J., McCabe, D.C., Wennberg, P.O., Sorooshian, A., Murphy, S.M. and Dalleska, N.F.: Effect of NOx level on secondary organic aerosol (SOA) formation from the photooxidation of terpenes. Atmospheric Chemistry and Physics, 7(19), 5159-5174, 2007.

Odum, J.R., Jungkamp, T.P.W., Griffin, R.J., Forstner, H.J.L., Flagan, R.C. and Seinfeld, J.H.: Aromatics, reformulated gasoline, and atmospheric organic aerosol formation. Environmental Science & Technology, 31(7), 1890-1897, 1997.

Park, S., Bretherton, C. S., and Rasch, P. J.: Integrating Cloud Processes in the Community Atmosphere Model, Version 5, J. Climate, 27, 6821-6856, 10.1175/Jcli-D-14-00087.1, 2014.

Randerson, J. T., Chen, Y., van der Werf, G. R., Rogers, B. M., and Morton, D. C.: Global burned area and biomass burning emissions from small fires, J. Geophys. Res.-Biogeo., 117, G04012, https://doi.org/10.1029/2012JG002128, 2012.

Riahi, K., Van Vuuren, D.P., Kriegler, E., Edmonds, J., O'neill, B.C., Fujimori, S., Bauer, N., Calvin, K., Dellink, R., Fricko, O. and Lutz, W.: The shared socioeconomic pathways and their energy, land use, and greenhouse gas emissions implications: an overview. Global Environmental Change, 42, pp.153-168, 2017.

Tosca, M. G., Randerson, J. T., and Zender, C. S.: Global impact of smoke aerosols from landscape fires on climate and the Hadley circulation, Atmos. Chem. Phys., 13, 5227-5241, 10.5194/acp-13-5227-2013, 2013.

Tost, H., Jöckel, P. and Lelieveld, J.: Lightning and convection parameterisations–uncertainties in global modelling. Atmospheric Chemistry and Physics, 7(17), 4553-4568, 2007.

Van der Werf, G.R., Randerson, J.T., Giglio, L., Collatz, G.J., Mu, M., Kasibhatla, P.S., Morton, D.C., DeFries, R.S., Jin, Y.V. and van Leeuwen, T.T.: Global fire emissions and the contribution of deforestation, savanna, forest, agricultural, and peat fires (1997–2009). Atmospheric chemistry and physics, 10(23), 11707-11735, 2010.

Zou, Y., Wang, Y., Ke, Z., Tian, H., Yang, J., and Liu, Y.: Development of a REgion-Specific ecosystem feedback Fire (RESFire) model in the Community Earth System Model, J. Adv. Model Earth Sy., https://doi.org/10.1029/2018MS001368, 2019.

Using CESM-RESFire to Understand Climate-Fire-Ecosystem Interactions and the Implications for Decadal Climate Variability

Yufei Zou[1†], Yuhang Wang[1], Yun Qian[2], Hanqin Tian[3], Jia Yang[4], Ernesto Alvarado[5]

[1]School of Earth and Atmospheric Sciences, Georgia Institute of Technology, Atlanta, GA 30332, USA.
[2]Atmospheric Sciences and Global Change Division, Pacific Northwest National Laboratory, Richland, WA 99354, USA.
[3]International Centre for Climate and Global Change Research, School of Forestry and Wildlife Sciences, Auburn University, AL 36849, USA.
[4]College of Forest Resources/Forest and Wildlife Research Center, Mississippi State University, MS 39762, USA.
[5]School of Environmental and Forest Sciences, University of Washington, Seattle, WA 98195, USA.
† Now at Pacific Northwest National Laboratory, Richland, WA 99354, USA.

Correspondence to: Yuhang Wang (yuhang.wang@eas.gatech.edu) and Yufei Zou (yufei.zou@pnnl.gov)

Abstract. Large wildfires exert strong disturbance to regional and global climate systems and ecosystems by perturbing radiative forcing as well as carbon and water balance between the atmosphere and land surface, while short- and long-term variations in fire weather, terrestrial ecosystems, and human activity modulate fire intensity and reshape fire regimes. The complex climate-fire-ecosystem interactions were not fully integrated in previous climate model studies, and the resulting effects on the projections of future climate change are not well understood. Here we use a fully interactive REgion-Specific ecosystem feedback Fire model (RESFire) that was developed in the Community Earth System Model (CESM) to investigate these interactions and their impacts on climate systems and fire activity. We designed two sets of decadal simulations using CESM-RESFire for present-day (2001-2010) and future (2051-2060) scenarios, respectively and conducted a series of sensitivity experiments to assess the effects of individual feedback pathways among climate, fire, and ecosystems. Our implementation of RESFire, which includes online land-atmosphere coupling of fire emissions and fire-induced land cover change (LCC), reproduces the observed Aerosol Optical Depth (AOD) from space-based Moderate Resolution Imaging Spectroradiometer (MODIS) satellite products and ground-based AErosol RObotic NETwork (AERONET) data and agrees well with carbon budget benchmarks from previous studies. We estimate the global averaged net radiative effect of both fire aerosols and fire-induced LCC at -0.59 ± 0.52 W m^{-2}, which is dominated by fire aerosol-cloud interactions (-0.82 ± 0.19 W m^{-2}), in the present-day scenario under climatological conditions of the 2000s. The fire-related net cooling effect increases by ~170% to -1.60 ± 0.27 W m^{-2} in the 2050s under the conditions of the Representative Concentration Pathway 4.5 (RCP4.5) scenario. Such considerably enhanced radiative effect is attributed to the largely increased global burned area (+19%) and fire carbon emissions (+100%) from the 2000s to the 2050s driven by climate change. The net ecosystem exchange (NEE) of carbon between the land and atmosphere components in the simulations increases by 33% accordingly, implying that biomass burning is an increasing carbon source at short-term timescales in the future. High-latitude regions with prevalent peatlands would be more vulnerable to increased fire threats due to climate change and the increase of fire aerosols could counter the projected decrease of anthropogenic aerosols due to air pollution control policies in many

Deleted: Understanding
Formatted: Left
Deleted: Using CESM-RESFire
Deleted: [2]Pacific
Deleted: yufeizou@gmail.com
Deleted: ¶
Deleted: included
Deleted: used
Deleted: reproduced
Deleted: agreed
Deleted: estimated
Deleted: was
Deleted: increased
Deleted: greatly
Deleted: was
Deleted: increased
Deleted: climate effects of the

regions. We also evaluate two distinct feedback mechanisms that are associated with fire aerosols and fire-induced LCC, respectively. On a global scale, the first mechanism imposes positive feedbacks to fire activity through enhanced droughts with suppressed precipitation by fire aerosol-cloud interactions, while the second one manifests as negative feedbacks due to reduced fuel loads by fire consumption and post-fire tree mortality and recovery processes. These two feedback pathways with opposite effects compete at regional to global scales and increase the complexity of climate-fire-ecosystem interactions and their climatic impacts.

Deleted: evaluated
Deleted: were
Deleted: .
Deleted: imposed
Deleted: feedback
Deleted: manifested
Deleted: feedback
Deleted: competed
Deleted: increased

1 Introduction

Large wildfires show profound impacts on human society and the environment with increasing trends in many regions around the world during recent decades (Abatzoglou and Williams, 2016;Barbero et al., 2015;Clarke et al., 2013;Dennison et al., 2014;Jolly et al., 2015;Westerling et al., 2006;Yang et al., 2011;Yang et al., 2015). They pose a great threat to the safety of communities in the vicinity of fire-prone regions and distant downstream areas by both destructive burning and increased health risks from fire smoke exposure. The global annual averaged premature deaths due to fire smoke exposure was estimated about 339,000 (interquartile range: 260,000-600,000) during 1997 to 2006 (Johnston et al., 2012), while the total cost of fire-related socioeconomic burden would surge much higher if other societal and environmental outcomes, such as morbidity of respiratory and cardiovascular diseases, expenditures of defensive actions and disutility, and ecosystem service damages, were taken into account (Fann et al., 2018;Hall, 2014;Richardson et al., 2012;Thomas et al., 2017). In addition to hazardous impacts on human society, fire also exerts strong disturbance to regional and global climate systems and ecosystems by perturbing radiation budget and carbon balance between the atmosphere and land surface. In return, these short-term and long-term changes in fire weather, terrestrial ecosystems, and human activity modulate fire intensity and reshape fire regimes in many climate change sensitive regions. These processes were not fully included in previous climate model studies, increasing uncertainties in the projections of future climate variability and fire activity (Flannigan et al., 2009;Hantson et al., 2016;Harris et al., 2016;Liu et al., 2018). Most fire-related climate studies used a one-way perturbation approach by examining a unidirectional forcing and response between climate change and fire activity without feedback. For instance, many historical and future-projected fire responses to climate drivers were mainly based on offline statistical regression or one-way coupled prognostic fire models in earth system models, while fire feedback to weather, climate, and vegetation was neglected (e.g., Abatzoglou et al., 2019;Flannigan et al., 2013;Hurteau et al., 2014;Liu et al., 2010;Moritz et al., 2012;Parks et al., 2016;Wotton et al., 2017;Young et al., 2017;Yue et al., 2013). The neglected feedback could affect regional to global radiative forcing, biogeochemical and hydrological cycles, and ecological functioning that may in turn modulate fire activity in local and remote regions (Harris et al., 2016;Liu, 2018;Pellegrini et al., 2018;Seidl et al., 2017;Shuman et al., 2017). Similarly, climate studies (e.g., Jiang et al., 2016;Tosca et al., 2013;Ward et al., 2012) that focused on climate responses to fire forcing used the same unidirectional approach but from an opposite perspective, in which they evaluated multiple fire impacts on climate systems through fire aerosols, greenhouse gases, and land albedo effects using climate sensitivity experiments with and without prescribed fire emissions as model inputs. However, possible fire activity and emission changes in response to these fire weather and climate variations were missing in such one-way perturbation modeling approaches.

Deleted: at
Deleted: These complex climate-fire-ecosystem interactions are further confounded by natural processes and human interferences.
Deleted: fixed

To tackle these problems, we developed a two-way coupled RESFire model (Zou et al., 2019) with online land-atmosphere coupling of fire-related mass and energy fluxes as well as fire-induced land cover change in CESM (hereafter as CESM-RESFire). CESM-RESFire performs well using either offline observation-/reanalysis-based atmosphere data or online simulated atmosphere, which is applied in this study to investigate the complex climate-fire-ecosystem interactions as well as to project future climate change with fully interactive fire disturbance. In this work, we use the state-of-the-science CESM-RESFire model to evaluate major climate-fire-ecosystem interactions through biogeochemical, biogeophysical, and hydrological pathways and to assess future changes of decadal climate variability and fire activity with consideration of these interactive feedback processes. We provide a brief model description and sensitivity experiment settings in Section 2 and present modeling results and analyses on radiative effects, carbon balance, and feedback evaluation in Section 3. Final conclusions and implications are followed in Section 4.

Deleted: performed

Deleted: were

Deleted: used

Deleted: feedback in

Deleted: provided

Deleted: presented

2 CESM-RESFire description, simulation setup, and benchmark data

2.1 Fire model and sensitivity simulation experiments

RESFire (Zou et al., 2019) is a process-based fire model developed in the CESM version 1.2 modeling framework that incorporates ecoregion-specific natural and anthropogenic constraints on fire occurrence, fire spread, and fire impacts in both the CESM land component—the Community Land Model version 4.5 (CLM4.5) (Oleson et al., 2013) and the atmosphere component—the Community Atmosphere Model version 5.3 (CAM5) (Neale et al., 2013). It is compatible with either observation/reanalysis-based data atmosphere or the CAM5 atmosphere model with online land-atmosphere coupling through aerosol-climate effects and fire-vegetation interactions. It includes two major fire feedback pathways: the atmosphere-centric fire feedback through fire-related mass and energy fluxes and the vegetation-centric fire feedback through fire-induced land cover change. These feedback pathways correspond to two key climate variables, radiative forcing and carbon balance, through which fires exert their major climatic and ecological impacts. Other features in CLM4.5 and CAM5, such as the photosynthesis scheme (Sun et al., 2012), the 3-mode modal aerosol module (MAM3; Liu et al., 2012), and the cloud microphysics (Morrison and Gettelman, 2008; Gettelman et al., 2008) and macrophysics (Park et al., 2014) schemes, allow for more comprehensive assessments of climate effects of fires through the interactions with vegetation and clouds. A simple treatment of secondary organic aerosols (SOA) is used in CAM5 to derive SOA formation from anthropogenic and biogenic volatile organic compounds (VOCs) with fixed mass fields (Table S1 in the Supplement). The total SOA mass is emitted as the SOA (gas) species from the surface and then condensation/evaporation of gas-phase SOA to/from different aerosol modes are calculated in the MAM3 module (Neale et al., 2013). The gas-phase photochemistry is not included in the CAM5 simulations, which precludes the possibility for evaluating chemistry-climate interactions. We also implement distribution mapping-based online bias corrections for key fire weather variables (i.e., surface temperature, precipitation, and relative humidity) to reduce negative influences of climate model biases in atmosphere simulation and projection. Fire plume rise is globally universal parameterized based on atmospheric boundary layer height (PBLH), fire radiative power (FRP), and Brunt-Väisälä frequency in the free troposphere (Sofiev et al., 2012). Please refer to Zou et al. (2019) for more detailed fire model descriptions and to Sofiev et al. (2012) for the fire plume rise

Deleted: MAM3

Deleted: scheme

Deleted:),

Deleted: We also implemented

Formatted: English (UK)

parameterization. To quantify the impacts of fire-climate interactions under different climatic conditions, we designed two groups of sensitivity simulations for present-day and future scenarios (Table 1). In each simulation group, we conducted one control run (CTRLx, where x=1 or 2 indicates the present-day or future scenario, respectively) and two sensitivity runs (SENSxA/B, where x is the same as that in CTRL runs and the notations of A and B are explained below). The CTRL runs were designed with fully interactive fire disturbance such as fire emissions with plume rise and fire-induced LCC with different boundary conditions for a present-day scenario (CTRL1; 2001-2010) and a moderate future emission scenario (CTRL2) of the Representative Concentration Pathway 4.5 (RCP4.5; 2051-2060), respectively. In each scenario, we turned off the atmosphere-centric feedback mechanisms (e.g., fire aerosol climate effects) in SENSxA simulations (where x=1 or 2) and then turned off both atmospheric-centric and vegetation-centric fire feedback (e.g., fire-induced LCC) in SENSxB simulations. Consequently, we estimated the atmosphere-centric impacts of fire emissions on radiative forcing in the present-day scenario (RCP4.5 future scenario) by comparing SENS1A (SENS2A) with CTRL1 (CTRL2). We also estimated the vegetation-centric impacts of fire-induced LCC on terrestrial carbon balance in the present-day scenario (RCP4.5 future scenario) by comparing SENS1B (SENS2B) with SENS1A (SENS2A). The net fire-related effects were evaluated by comparing CTRL runs with SENSxB runs as both fire feedback mechanisms were turned off in the SENSxB runs. Using these sensitivity experiments, we are able to evaluate two-way climate-fire-ecosystem interactions under the same integrated modeling framework that is not possible in one-way perturbation studies considering either climate impacts on fires (Kloster et al., 2010;Kloster et al., 2012;Thonicke et al., 2010) or fire feedback to climate (Jiang et al., 2016;Li et al., 2014;Ward et al., 2012;Yue et al., 2015;Yue et al., 2016).

Deleted: A new fire plume rise scheme (Ke et al., 2019) is under development and will be implemented in CESM-RESFire in the future. …

Deleted: evaluated

Deleted: was

2.2 Model input data

We used the spun-up files from previous long-term runs (Zou et al., 2019) as initial conditions for the present-day experiments (CTRL1 and SENS1A/B). The boundary conditions including the prescribed climatological (1981-2010 average) sea surface temperature and sea ice data for the present-day scenario were obtained from the Met Office Hadley Centre (HadISST) (Rayner et al., 2003). Similarly, the nitrogen and aerosol deposition rates were also prescribed from a time-invariant spatially varying annual mean file for 2000 and a time-varying (monthly cycle) globally-gridded deposition file, respectively, as the standard datasets necessary for the present-day CAM5 simulations (Hurrell et al., 2013). The climatological 3-hourly cloud-to-ground lightning data via bilinear interpolation from NASA LIS/OTD grid product v2.2 (http://ghrc.msfc.nasa.gov) 2-hourly lightning frequency data and the world population density data were fixed at the 2000 levels for all the present-day simulations. The non-fire emissions from anthropogenic sources (e.g., industrial, domestic and agriculture activity sectors) in the present-day scenario were from the emission dataset (Lamarque et al., 2010) representing year 2000 for the Fifth Assessment Report of the Intergovernmental Panel on Climate Change (IPCC AR5). Emissions of natural aerosols such as dust and sea salt were calculated online (Neale et al., 2013), while vertically resolved volcanic sulfur and dimethyl sulfide (DMS) emissions were prescribed from the AEROCOM emission dataset (Dentener et al., 2006). Emission fluxes for the 5 VOC species (isoprene, monoterpenes, toluene, big alkenes, and big alkanes) to derive SOA mass yields were prescribed from the MOZART-2 dataset (Horowitz et al., 2003). For fire emissions, we replaced the prescribed GFED2 fire emissions

Deleted: in the

Deleted: We replaced the old prescribed GFED2 fire emissions (van der Werf et al., 2006) in

(van der Werf et al., 2006) from the default offline emission data with online coupled fire emissions generated by the RESFire model in the CTRL runs. We then decoupled online simulated fire emissions in the SENS1A runs, in which fire emissions were not transported to the CAM5 atmosphere model, to isolate the atmosphere-centric impacts of fire-climate interactions. In both CTRL1 and SENS1A experiments, we allowed the semi-static historical LCC data for the year 2000 from the version 1 of the Land-Use History A product (LUHa.v1) (Hurtt et al., 2006) to be affected by post-fire vegetation changes (Zou et al., 2019). We then used the fixed LCC data for the year 2000 in the SENS1B run and compared two SENS1 runs (SENS1A-SENS1B) to evaluate the vegetation-centric fire impacts on terrestrial ecosystems and carbon balance in the 2000s.

For the future scenario experiments, we replaced all the present-day datasets with the RCP4.5 projection datasets including the initial conditions and prescribed boundary conditions of global SST and sea ice data in 2050, the cyclical non-fire emissions and deposition rates fixed in 2050 under the RCP4.5 scenario, and the annual LCC data for the RCP4.5 transient period in 2050 based on the Future Land-Use Harmonization A products (LUHa.v1_future) (Hurtt et al., 2006). All these datasets were described in the technical note of CAM5 (Neale et al., 2013) and stored on the Cheyenne computing system (CISL, 2017) at the National Center for Atmospheric Research (NCAR)-Wyoming Supercomputing Center (NWSC). It is worth noting that we used the present-day demographic data and observation-based climatological lightning data in the future scenario given pathway-dependence and great uncertainties in future projections of these inputs (Clark et al., 2017;Riahi et al., 2017;Tost et al., 2007;). In other words, we did not consider the influence of fire ignition changes associated with human activity or lightning flash density in our future projection simulations but focused on broad impacts of future climate change on fuel loads and combustibility as well as fire weather conditions.

The global mean greenhouse gas (GHG) mixing ratios in the CAM5 atmosphere model were fixed at the 2000-year levels (CO_2: 367.0 ppmv; CH_4:1760.0 ppbv; N_2O:316.0 ppbv) in all present-day experiments and they were replaced by the prescribed RCP4.5 projection datasets with the well-mixed assumption and monthly variations in the future scenarios. These GHG mixing ratios were then passed to the CLM4.5 land model in all sensitivity experiments. In return, the land model provided the diagnostics of the balance of all carbon fluxes between net ecosystem production (NEP, g C m^{-2} s^{-1}, positive for carbon sink) and depletion from fire emissions, landcover change fluxes, and carbon loss from wood products pools, and then the computed net CO_2 flux was passed to the atmosphere model in forms of net ecosystem exchange (NEE, g C m^{-2} s^{-1}). Though fire emissions could perturb the value of NEE at short-term scales, it is often assumed that fire is neither a source nor a sink for CO_2 since fire carbon emissions are offset by carbon absorption of vegetation regrowth over long-term scales (Bowman et al., 2009). Therefore, we did not consider the radiative effect of fire-related GHGs in our sensitivity experiments. This kind of "concentration-driven" simulations with prescribed atmospheric CO_2 concentrations for a given scenario have been used extensively in previous fire-climate interaction assessments (e.g., Kloster et al., 2010;Li et al., 2014;Thonicke et al., 2010) and most of the RCP simulations (Ciais et al., 2013).

Deleted: perturbed
Deleted: through
Deleted: same population density
Deleted: with the present-day scenario
Deleted: .
Deleted: demographic
Deleted: frequency changes
Deleted: except lightning
Deleted: greenhouse gases (
Deleted:)
Deleted:

2.3 Model evaluation benchmarks and datasets

Multiple observational and assimilated datasets were applied to evaluate the modeling performance regarding radiative forcing. We collected space-based column aerosol optical depth (AOD) from the level-3 MODIS Aqua monthly global product (MYD08_M3, Platnick et al., 2015) and ground-based version 3 aerosol optical thickness (AOT) level 2.0 data from the Aerosol Robotic Network (AERONET, https://aeronet.gsfc.nasa.gov/) project for comparison with the model simulated AOD data at 550 nm. The AERONET AOT at 550 nm were interpolated by estimating Ångström exponents based on the measurements taken at two closest wavelengths at 500 nm and 675 nm (see the Supplement for details). We then followed the Ghan method (Ghan, 2013) to estimate fire aerosol radiative effects (RE_{aer}) on the planetary energy balance in terms of aerosol-radiation interactions (RE_{ari}), aerosol-cloud interactions (RE_{aci}), and fire aerosol-related surface albedo change (RE_{sac}) in Eq. (1). The radiative effect related to fire-induced land cover change (RE_{lcc}) was estimated by comparing shortwave radiative fluxes at the top-of-atmosphere (TOA) between SENSxA (with fire-induced LCC) and SENSxB (without fire-induced LCC) experiments. By summing up all these terms, we estimated the fire-related net radiative effect (RE_{fire}) as the shortwave radiative flux difference between CTRLx (with fire aerosols and fire-induced LCC) and SENSxB (without fire aerosols and fire-induced LCC) experiments:

$$\begin{gathered} RE\ of\ interaction\ of\ radiation\ with\ fire\ aerosol{:}\ RE_{ari} = \Delta(F - F_{clean}) \\ RE\ of\ interaction\ of\ clouds\ with\ fire\ aerosol{:}\ RE_{aci} = \Delta(F_{clean} - F_{clear,clean}) \\ RE\ of\ surface\ albedo\ change\ induced\ by\ fire\ aerosol{:}\ RE_{sac} = \Delta F_{clear,clean} \\ net\ RE\ of\ fire\ aerosol{:}\ RE_{aer} = RE_{ari} + RE_{aci} + RE_{sac} = F_{CTRLx} - F_{SENSxA} \\ RE\ of\ fire\ induced\ land\ cover\ change{:}\ RE_{lcc} = F_{SENSxA} - F_{SENSxB} \\ net\ RE\ of\ fire{:}\ RE_{fire} = RE_{aer} + RE_{lcc} = F_{CTRLx} - F_{SENSxB} \end{gathered} \quad (1)$$

where Δ is the difference between control and sensitivity simulations, F is the shortwave radiative flux at the TOA, F_{clean} is the radiative flux calculated as an additional diagnostics from the same simulations but neglecting the scattering and absorption of solar radiation by all aerosols, and $F_{clear,clean}$ is the flux calculated as additional diagnostic but neglecting scattering and absorption by both clouds and aerosols. The surface albedo effect is largely the contribution of changes in surface albedo induced by fire aerosol deposition and land cover change, which is small but non-negligible in some regions (Ghan, 2013). We used similar modeling settings including the 3-mode modal aerosol scheme (MAM3) (Liu et al., 2012) and the Snow, Ice, and Aerosol Radiative (SNICAR) module (Flanner and Zender, 2005) and compared our online coupled fire modeling results against previous offline prescribed fire modeling studies (Jiang et al., 2016;Ward et al., 2012) in the next section.

We also examined the modeling performance on burned area and terrestrial carbon balance such as fire carbon emissions, gross primary production (GPP, g C m^{-2} s^{-1}, positive for vegetation carbon uptake), net primary production (NPP, g C m^{-2} s^{-1}, positive for vegetation carbon uptake), net ecosystem productivity (NEP, g C m^{-2} s^{-1}, positive for net ecosystem carbon uptake), and net ecosystem exchange (NEE, g C m^{-2} s^{-1}, positive for net ecosystem carbon emission). The model simulated burned area and fire carbon emissions were evaluated against the satellite based GFED4.1s datasets (Giglio et al., 2013;Randerson et al., 2012;van der Werf et al., 2017), and these carbon budget related variables were calculated in Eqs. (2) and (3) and compared with the MODIS primary production products (Zhao et al., 2005;Zhao and Running, 2010), previous modeling results used for terrestrial model comparison projects

Deleted: supplement

Deleted: Ghan's

Deleted: $fire\ aerosol - radiation\ interaction\ RE{:}\ RE_{ari} =$ $fire\ aerosol - cloud\ interaction\ RE{:}\ RE_{aci} = \Delta(F_{cle}$ $fire\ aerosol - related\ surface\ albedo\ change\ RE{:}\ RI$ $fire\ aerosol\ net\ RE{:}\ RE_{aer} = RE_{ari} + RE_{aci} + RE_{sac} =$ $fire - induced\ land\ cover\ change\ RE{:}\ RE_{lcc} = F_{SE}$ $fire - related\ net\ RE{:}\ RE_{fire} = RE_{aer} + RE_{lcc} = F_{c}$,→→→→(1)¶

Deleted: nonnegligible

Deleted: areas

Deleted: areas

(Piao et al., 2013) and the IPCC AR5 report (Ciais et al., 2013), and the global carbon budget assessment (Le Quere et al., 2013) by the broad carbon cycle science community.

$$\mathrm{GPP} = \mathrm{NPP} + R_a = (\mathrm{NEP} + R_h) + R_a, \quad (2)$$

$$\mathrm{NEE} = C_{fe} + C_{lh} - \mathrm{NEP} = C_{fe} + C_{lh} + R_h + R_a - \mathrm{GPP}, \quad (3)$$

where R_a is the total ecosystem autotrophic respiration (g C m^{-2} s^{-1}), R_h is the total heterotrophic respiration (g C m^{-2} s^{-1}), C_{fe} is the fire carbon emissions (g C m^{-2} s^{-1}), and C_{lh} is the carbon loss (g C m^{-2} s^{-1}) due to land cover change, wood products, and harvest.

3 Modeling results and discussion

3.1 Evaluation of fire-related radiative effects

Figure 1 shows the comparison of the model simulated 10-year annual averaged column AOD at 550nm from CTRL1 and space-based AOD from MODIS aboard the Aqua satellite. It's noted that both AOD data result from all sources including fire and non-fire emissions, and significant differences exist in specific regions due to large biases in model emission inputs and aerosol parameterization. In the MODIS AOD data, the most noticeable hotspot regions include eastern China, South Asia such as India, and Africa. The first two regions are contributed mostly by anthropogenic emissions, while the last one is dominated by fire emissions. Since the non-fire emissions used in CAM5 simulations are 2000-based (Lamarque et al., 2010) and low biased comparing to rapid emission increases in many Asian developing countries (Kurokawa et al., 2013), the simulated hotspot regions in East and South Asia are not as appreciable as those observed in the remote sensing data. The model results also show underestimation in rainforests over South America and Central Africa, where large fractions of aerosols are contributed by primary and secondary organic aerosols from biogenic sources and precursors (Gilardoni et al., 2011) that are missing in the simulation. Another possible cause for the underestimation problem is underrepresented burning activity due to deforestation and forest degradation and consequently underestimated fire aerosols emissions in these regions. The AOD simulations over tropical savanna regions with pervasive biomass burning activities are also lower than the satellite observations, which might be attributable to both underestimated online fire emissions and too strong wet scavenging of primary carbonaceous aerosols in the CAM5-MAM3 model (Liu et al., 2012). The CAM5 model overestimates dust emissions significantly with some spuriously high AOD hotspots emerging over the Sahara, Arabian, South Africa, and Central Australia desert regions. This dust AOD overestimation problem was also found in a previous dust modeling study using the release version of the CAM5-MAM3 model (Albani et al., 2014).

To further evaluate the fire-related AOD modeling performance, we compare the difference between CTRL1 and SENS1A to isolate aerosol contributions from fire sources in Fig. 2. The spatial distribution of fire-related AOD clearly highlighted African savanna as a major biomass burning region. We also compare monthly AOD at six fire-prone regions with AERONET observations to get a better understanding of temporal variations of fire aerosols. Most sites show strong seasonal variations in monthly AOD as observed by AERONET, and the CESM-RESFire model well capture fire seasonality in these regions. Generally, the model AOD results are at the lower ends of the uncertainty ranges of ground-based observations in most regions due to limited spatial representativeness of coarse model grid

Deleted: budge
Deleted: Fire
Deleted: We compared
Deleted: in Fig. 1
Deleted: resulted
Deleted: existed
Deleted: were
Deleted: were
Deleted: were
Deleted: However,
Deleted: model well captured the high AOD
Deleted: the Northern and Southern Hemispheres of Africa
Deleted: the dominant role of
Deleted: emissions in this region. It's also noticeable that
Deleted: overestimated
Deleted: AOD
Deleted: studies (Ridley
Deleted: 2016
Deleted: compared
Deleted: compared
Deleted: in situ
Deleted: showed
Deleted: captured
Deleted: were
Deleted: in situ

resolution and fire emissions, especially over African savannas like Ilorin (Fig. 2e) and Southeast Asian rainforests like Jambi (Fig. 2g) where agricultural and deforestation related burning activity prevails.

Lastly, we estimate present-day radiative effects of fire aerosols and fire-induced land cover change and compare the results with previous studies in Fig. 3 and Table 2. The radiative effect of fire aerosol-radiation interactions (RE_{ari}) is most prominent in tropical Africa and downwind Atlantic Ocean areas as well as South America and eastern Pacific. High-latitude regions like eastern Siberia also show significant positive radiative effects due to fire emitted light absorbing aerosols such as black carbon (BC). The land-sea contrast of radiative warming and cooling effects over Africa and South America are attributed to differences of cloud cover fractions over land and ocean areas (Jiang et al., 2016). In these regions, cloud fractions and liquid water path are much larger over downwind ocean areas than land areas during the fire season. Cloud reflection of solar radiation strongly enhances light absorption by fire aerosols residing above low-level marine clouds (Abel et al., 2005; Zhang et al., 2016).

The radiative effect of fire aerosol-cloud interactions (RE_{aci}) shows generally cooling effects in most regions due to scattering and reflections by enhanced cloudiness, and these cooling effects are more pervasive over high-latitude regions such as boreal forests in North America and eastern Siberia. The land-sea contrast of radiative effects emerges again in the vicinity of Africa and South America, but the signs of the contrasting effect related with aerosol-cloud interactions are opposite to these from aerosol-radiation interactions. The large amounts of fire aerosols suppress low-level clouds over the African land region by stabilizing the lower atmosphere through reduction of radiative heating of the surface. However, fire aerosols increase cloud cover and brightness in the downwind Atlantic Ocean areas because they increase the number of cloud condensation nuclei and the larger cloud droplet number density reduce cloud droplet sizes (Lu et al., 2018; Rosenfeld et al., 2019; Fig. S1 in the Supplement). The radiative effect of fire aerosol-related surface albedo change (RE_{sac}) shows contrasting radiation effects with strong warming effects over most Arctic regions caused by deposition of light-absorbing aerosol over ice and snow and reduction of surface albedo, but moderate cooling effects in boreal land regions such as Canada and eastern Siberia, which are related to fire aerosol-induced snowfall and snow cover change and associated surface albedo change (Ghan, 2013; Fig. S2 in the Supplement). Besides spatial heterogeneity in fire-induced radiative effects, these radiative effects also show significant temporal variations that are related with fire seasonality. Figure 4 shows zonal averaged time-latitude cross sections of fire aerosol emissions and fire-induced changes in clouds and radiative effects. Massive fire carbonaceous emissions shift from the Northern Hemisphere tropical regions in boreal winter to the Southern Hemisphere tropical regions in boreal summer, when similar amounts of fire emissions are also observed in boreal mid- and high-latitude regions (Fig. 4a/b). Fire aerosols greatly increase cloud condensation nuclei (CCN, Fig. 4c) and cloud droplet number concentrations (CDNUMC, Fig. 4d) in these regions, while the increase in cloud water path (CWP, Fig. 4e) and low cloud fraction (CLDLOW, Fig. 4f) are more significant in boreal high-latitude regions than in the tropics. The low solar zenith angle in high-latitude regions enhances solar radiation absorption by light-absorbing aerosols and results in stronger changes in radiative effects by aerosol-radiation interactions during boreal summer (Fig. 4g). In the meantime, increased CWP and CLDLOW in high-latitude regions also lead to much stronger cooling effects by aerosol-cloud interactions (RE_{aci}) (Fig. 4h), which overwhelm the increase in RE_{ari}. These modeling results based on the online coupled RESFire model show similar spatiotemporal patterns with these in Jiang et al. (2016), which used

Deleted: estimated
Deleted: compared
Deleted: was
Deleted: showed
Deleted: radiative
Deleted: were
Deleted: over ocean areas
Deleted: showed
Deleted: were
Deleted: Similar
Deleted: emerged
Deleted: contrast
Deleted: were
Deleted: with
Deleted: showed similarly spatial patterns with
Deleted: were
Deleted: snow precipitation and
Deleted: showed
Deleted: were
Deleted: shifted
Deleted: were
Deleted: increased
Deleted: were
Deleted: enhanced
Deleted: resulted
Deleted: leaded
Deleted: overwhelmed
Deleted: (2016) that were

the same version of the CAM5 atmosphere model with a 4-mode modal aerosol module (MAM4) that was driven by offline prescribed fire emissions.

In general, the 10-year averaged global mean values and standard deviations of interannual variations for fire aerosol-related RE_{ari}, RE_{aci}, and RE_{sac} in the 2000s are -0.003 ± 0.013 W m^{-2}, -0.82 ± 0.19 W m^{-2}, and 0.19 ± 0.61 W m^{-2}, respectively, and fire-induced RE_{lcc} is 0.04 ± 0.38 W m^{-2}. After combining all these forcing terms, we estimate a net RE_{fire} of -0.59 ± 0.51 W m^{-2} for the present-day scenario that is larger than the estimate of -0.55 W m^{-2} in the previous fire radiative effect studies (Jiang et al., 2016;Ward et al., 2012). It is noted that both Ward et al. (2012) and Jiang et al. (2016) used prescribed fire emissions from CLM3 model simulations (Kloster et al., 2010;Kloster et al., 2012) and GFED datasets (Giglio et al., 2013;Randerson et al., 2012), respectively, for their uncoupled fire sensitivity simulations. The annual fire carbon emissions used by Ward et al. (2012) ranged from 1.3 Pg C yr^{-1} for the present-day simulation to 2.4 Pg C yr^{-1} for the future projection with ECHAM atmospheric forcing, while the fire BC, POM and SO_2 emissions used by Jiang et al. (2016) were based on the GFEDv3.1 dataset with an annual averaged fire carbon emission of 1.98 Pg C yr^{-1} (Randerson et al., 2012). Their fire emissions are lower than the RESFire model simulation of 2.6 Pg C yr^{-1} (Table 3) in this study, which contribute to the differences in the estimates of fire aerosol radiative effects. It is also worth noting that all fire emissions were released into the lowest CAM level as surface sources by Ward et al. (2012), and a default vertical profile of fire emissions based on the AEROCOM protocol (Dentener et al., 2006) was used by Jiang et al. (2016) in their CAM5 simulations. In our simulations, we used a simplified plume rise parameterization (Sofiev et al., 2012) based on online calculated fire burning intensity (FRP) and atmospheric stability conditions (PBLH and Brunt-Väisälä frequency) in CESM-RESFire and applied vertical profiles with diurnal cycles to the vertical distribution of fire emissions. The simulations of annual median heights of fire plumes for the present-day and RCP4.5 future scenarios are shown in Fig. 5. Previous observation-based injection height studies suggested that only 4–12% fire plumes could penetrate planetary boundary layers with most fire plumes stay within the near surface atmosphere layers (val Martin et al., 2010). Our plume-rise simulation results agree with these estimates, though a quantitative comparison is beyond the scope of this study because of the inconsistency between simulated and actual meteorological conditions. It is also noted that there is no systematic change in plume rise height distributions between the RCP4.5 future scenario and present-day scenarios, both of which show most fire plumes (~80%) rise less than 1000 m. Comparing to surface released fire emissions in previous studies (Ward et al., 2012), our higher elevated fire plumes affect the vertical distribution and lifetime of fire aerosols and further influence regional radiative effects after long-range transport of fire aerosols.

3.2 Fire-related disturbance to carbon balance

In addition to the atmosphere-centric fire-induced radiative effects, we also quantify the vegetation-centric terrestrial carbon budget changes to evaluate fire disturbance to terrestrial ecosystems. We use the previous model inter-comparison studies and the latest GFEDv4.1s datasets as evaluation benchmarks and examine fire-related metrics including global burned area and fire carbon emissions (Fig. 6 and Table 3). We also collect global scale GPP, NPP, and NEE from previous literatures (Ciais et al., 2013; Piao et al., 2013;Zhao and Running, 2010) to compare with our simulation results (Table 3). The RESFire model performs well in global burned area and fire carbon emissions driven

Deleted: were
Deleted: was
Deleted: estimated
Deleted: were
Deleted: might result in
Deleted: AeroCom
Deleted: online calculated
Deleted: were
Deleted: ;Ke et al., 2019
Deleted: agreed
Deleted: was
Deleted: showed
Deleted: affected
Deleted: influenced
Deleted: Lastly, we compared the future scenario results with the present-day conditions in Table 2, which suggests a 171% increase of net fire aerosol and land cover change radiative effects from -0.59 ± 0.51 W m^{-2} in the present-day scenario to -1.60 ± 0.27 W m^{-2} in the RCP4.5 future scenario. Such enhanced negative radiative forcing is dominated by the increased RE_{aci} of fire aerosol-cloud interactions that is much larger than the CCSM future projection results (+51%) in Ward et al. (2012). It is noted that the net estimate of fire radiative forcing changes in Ward et al. (2012) included other offline-based fire climate effects such as fire-related GHGs impacts and climate-biogeochemical cycle feedback, which could dampen or strengthen the cooling effect of fire aerosols.
Deleted: evaluated
Deleted: .
Deleted: used
Deleted: examined
Deleted: collected
Deleted: performed

by either offline observation-/reanalysis-based CRUNCEP atmosphere data (RESFire_CRUNCEP) and online CAM5 simulated atmosphere data after bias corrections (RESFire_CAM5c). The annual averaged burned area results of both RESFire_CRUNCEP (508 ± 15 Mha yr^{-1}) and RESFire_CAM5c (472 ± 14 Mha yr^{-1}) are very close to the GFEDv4.1s benchmark value of 510 ± 27 Mha yr^{-1}, while the default fire model in CLM (322 Mha yr^{-1}) is significantly low biased. For fire carbon emissions, the offline RESFire_CRUNCEP result (2.3 ± 0.2 Pg C yr^{-1}) agrees well with the GFEDv4.1s benchmark of around 2.2 ± 0.4 Pg C yr^{-1}, and the online RESFire_CAM5c result shows a 18% higher value (2.6 ± 0.1 Pg C yr^{-1}) than the benchmark. Since the GFED emission datasets are low biased due to low satellite detection rates for small fires under canopy and clouds, previous fire studies (Johnston et al., 2012;Ward et al., 2012) rescaled fire emissions in their practice for climate and health impact assessment. Here, a moderate increase in online estimated fire carbon emissions would reduce the need for fire emission rescaling. Such difference is also consistent with the changes in different versions of the GFED datasets, which show a 11% increase of global fire carbon emissions in the latest GFED4s as compared with the old GFED3 for the overlapping 1997-2011 time period (van der Werf et al., 2017). This increased global fire carbon emissions in the GFED4s dataset result from a substantial increase in global burned area (+37%) due to inclusion of small fires and a modest decrease in mean fuel consumption (-19%) according to van der Werf et al. (2017). Since carbon emissions from deforestation fires and other land use change processes are a key component to estimate global carbon budget (Le Quere et al., 2013), improved fire emission estimation would benefit carbon budget simulation in the land model.

We then compare the CLM simulated carbon budget variables such as GPP and NEE against 10 process-based terrestrial biosphere models that were used for the IPCC fifth Assessment Report (Piao et al., 2013). Both the offline and online CLM GPP results are around 142 Pg C yr^{-1}, which are higher than the MODIS primary production products (MOD17) of 109.29 Pg C yr^{-1} (Zhao et al., 2005) and near the upper bound of ensemble modeling results (133 ± 15 Pg C yr^{-1}) (Piao et al., 2013). Such high GPP estimation leads to ~11% higher NPP in the CLM simulations than the MODIS global average annual NPP product of 53.5 Pg C yr^{-1} from 2001 to 2009 (Zhao and Running, 2010) as well as the old modeling result (54 Pg C yr^{-1}) based on the default fire model in CLM developed by Li et al. (2013;2014) (hereafter as CLM-LL2013). These differences may result from the different atmosphere forcing data used to drive the CLM land model. However, the NEE results based on the CESM-RESFire model are consistent with the benchmarks from the IPCC AR5 (Ciais et al., 2013) and ensemble modeling results (Piao et al., 2013), indicating a good land modeling performance with online fire disturbance in CESM.

After the evaluation of carbon budget in the CLM land model, we further decompose the components in NEE and compare the new CESM-RESFire simulation results with previous fire model simulations by Li et al. (2014). Following their experiment setting in Li et al. (2014), we isolate fire contributions to each carbon budget variables by differencing the fire-on and fire-off experiments driven by the CRUNCEP data atmosphere in Table 4. We find a 58% increase in fire-induced NEE variations simulated by CESM-RESFire than CLM-LL2013. This increase is attributed to enhanced fire emissions and suppressed NEP in CESM-RESFire. As discussed in the previous section, CESM-RESFire simulates higher annual averaged fire carbon emissions (2.08 Pg C yr^{-1}) than CLM-LL2013 (1.9 Pg C yr^{-1}), which contributes 31% of the difference in their NEE changes. Furthermore, CESM-RESFire simulates smaller NEP changes due to fire disturbance, which is attributable to fire-induced land cover change in RESFire. Fire-induced

Deleted: compared

Deleted: decomposed

Deleted: compared

Deleted: isolated

Deleted: found

Deleted: was

Deleted: simulated

Deleted: contributed

Deleted: simulated

Deleted: could be

Deleted: We considered fire

whole plant mortality and post-fire vegetation recovery are implemented in the new CESM-RESFire model (Zou et al., 2019), both of which are not included in the default CLM-LL2013 model. The newly incorporated fire-induced land cover change would influence ecosystem productivity and respiration as shown by carbon budget variables in Table 4. Specifically, the fire-induced whole plant mortality and recovery would moderate the variations in ecosystem productivity and respiration and further suppress fire-induced NEP changes. The suppressed NEP change explains 52% of the total difference between CESM-RESFire and CLM-LL2013 in simulated NEE changes.

Similar suppression effects of fires on NEP were also found in Seo and Kim (2019), in which they used the CLM-LL2013 fire model but enabled the dynamic vegetation (DV) mode to simulate post-fire vegetation changes. Though the DV mode of the CLM model is capable of simulating vegetation dynamics, considerable biases exist in the online simulation of land cover change by the coupled CLM-DV model (Quillet et al., 2010) and may undermine the interpretation of fire-related ecological effects. For instance, the global fractions of bare ground and needleleaf trees in the CLM-DV simulations are much larger than these in the non-DV (BGC only) simulation in Seo and Kim (2019), while the fractions of shrub and broadleaf trees with active DV are less than these without DV regardless of whether fire disturbance are included or not in the simulations. These biases could distort ecosystem properties such as primary production and carbon exchange as well as fire-related ecological effects.

Similar to fire-related radiative effects, we examine changes of carbon budget variables in the RCP4.5 future scenario in Table 5 and Fig. 7. The global burned area increases by 19% from the present-day scenario in CTRL1 (464 $\pm$ 19 Mha yr^{-1}) to the RCP4.5 future scenario in CTRL2 (551 $\pm$ 16 Mha yr^{-1}) (Fig. 7a). Accordingly, the annual averaged fire carbon emission increases by 100% from 2.5 $\pm$ 0.1 Pg C yr^{-1} at present to 5.0 $\pm$ 0.3 Pg C yr^{-1} in the future (Fig. 7b). This increase is larger than a previous CLM simulated result of 25%~52% by Kloster et al. (2010;2012), which might result from different climate sensitivity between CESM-RESFire and the old fire model in CLM. It's noted that recent satellite-based studies found decreasing trends in burned area over specific regions such as Northern Hemisphere Africa driven by human activity and agricultural expansion (Andela and van der Werf, 2014; Andela et al., 2017). Though we mainly focus on fire-climate interactions without consideration of human impacts in this study, the RESFire model is capable of capturing the anthropogenic interference on fire activity and reproducing observation-based long-term trends of regional burning activity driven by climate change and human factors (Zou et al., 2019). The carbon budget variables including GPP, NEP, and NEE increase by 4%, 7%, and 33%, respectively (Fig. 7c-d). These carbon variables affect terrestrial ecosystem productivity as well as fuel load supply for biomass burning, which further modulate fire emissions that lead to discrepancies between burned area and emission changes. For instance, most decreasing changes in burned area occur in tropical and subtropical savannas and grasslands, while significant increasing changes are evident in boreal forest and tropical rainforests of Southeast Asia (Fig. 7a). This spatial shift of burning activity from low fuel loading areas (e.g., grassland) to high fuel loading areas (e.g., forest) greatly amplifies the changes in fire emissions due to boosted fuel consumption. The complex climate-fire-ecosystem interactions will be discussed in the next section.

Deleted: were

Deleted: explained

Deleted: were

Deleted: were

Deleted: were

Deleted: examined

Deleted: increased

Deleted: increased

Deleted: -LL2013

Deleted: focused

Deleted: reproducing

Deleted: as observed from the space

Deleted: increased

Deleted: occurred

Deleted: were

Deleted: amplified

3.3 Simulations of climate-fire-ecosystem interactions using CESM-RESFire

In the last section, we find a 19% increase of global burned area in the RCP4.5 future scenario comparing with the present-day scenario. We then examine spatial distributions and driving factors of this change in Fig. 8. The fire ignition distribution shows heterogeneous changes with significant increases in boreal forest regions over Eurasia as well as rainforest regions in South America but decreases in South American savanna and African rainforests and savanna. These changes in fire ignition are mainly driven by changes in fuel combustibility as shown by fire combustion factors (Fig. 8b), which are computed using fire weather conditions including 10-day running means of surface air temperature, precipitation, and soil moisture (Zou et al., 2019). The spatial distribution changes of fire spread (Fig. 8c) shows similar but more apparent patterns of increased fire spread rates over most regions except savanna and rainforests in Africa and South America, which are attributed to the changes in fire spread factors (Fig. 8d). These fire spread factors depend on surface temperature, relative humidity, soil wetness, and wet canopy fractions that modulate fuel moisture and fire spread rates in the model (Zou et al., 2019). The burned area changes are driven by changes of fire weather conditions affecting both fire ignition and fire spread, with a global spatial correlation coefficient of 0.4 between differences in fractional burned area (Fig. 7a) and fire counts (Fig. 8a) and of 0.38 between burned area (Fig. 7a) and fire spread rates (Fig. 8c). These burning activity changes found in this study also agree quite well with previous long-term projections based on an empirical statistical framework and a multi-model ensemble of 16 GCMs, in which they found good model agreement on increasing fire probabilities (~62%) at mid- to high-latitudes as well as decreasing fire probabilities (~20%) in the tropics (Moritz et al., 2012).

To understand the changes in specific fire weather variables, we compare the differences of surface air temperature, total precipitation rates, relative humidity, and surface wind speed between the future (CTRL2) and present-day (CTRL1) scenarios in Fig. 9. As expected in a modest warming scenario, the global annual mean temperature is projected to increase by 1.7 °C on average with pervasive warming over land areas (Fig. 9a). The temperature increases are stronger in high latitude regions like Alaska, northern Canada, and Antarctica as well as Australia. Meanwhile, hydrological conditions also undergo significant but nonhomogeneous changes in many regions in the projection, with hot and dry weather conditions favorable for fire in Australia, Southeast Asia, Central America, and the northern coast of South America (Fig. 9b and 9c). Most of these regions also show increased surface wind speed that is conducive to faster fire spread (Fig. 9d). Since these variations in fully coupled CTRL experiments can be induced by either global warming driven weather changes or fire feedback, we further decompose the total changes into two components: one without fire feedback (i.e., SENS2B-SENS1B) and the other purely by fire feedback (i.e., (CTRL2-CTRL1)-(SENS2B-SENS1B)). We show the fire induced weather changes in Fig. 10 and these without fire feedbacks in Fig. S3 in the Supplement. It is clear that the majority of the changes in fire weather conditions is driven by atmospheric conditions associated with global warming since the spatial patterns in Fig. 9 and Fig.S3 almost resemble each other over most land regions. However, fire feedbacks also exert nonnegligible effects to local and remote weather conditions that manifest as positive or negative feedback mechanisms to regional fire activities. For instance, Australia shows increased temperature (Fig. 10a) and surface wind speed (Fig. 10d), and decreased precipitation (Fig. 10b) and relative humidity (Fig. 10c) induced by fire, which are consistent with these changes without fire feedbacks (Fig. S3 in the Supplement) or the total changes (Fig. 9). In contrast, most Eurasian regions show decreased temperature (Fig.

Deleted: found

Deleted: compared to

Deleted: examined driving factors and

Deleted: increase

Deleted: ,

Deleted: ,

Deleted:).

Deleted: fire spread

Deleted: middle- to high-latitude

Deleted: but decreased fire spread rates over tropical regions, which is…

Deleted:) modulated by

Deleted: precipitation, and

Deleted: mainly

Deleted: changes as suggested by

Deleted: rate variations because the increasing and decreasing areas…

Deleted: resemble the spatial pattern in fire spread rate changes

Moved down [1]: 8c).

Deleted: In other words, fire weather changes dominate

Moved (insertion) [1]

Deleted: changes in the future and determine the changing tendencies of burning severity in these fire-prone regions.

Deleted: To understand changes in specific fire weather variables, we compared the differences of surface wind speed, surface temperature, rain precipitation and snow precipitation in Fig. 9. Most statistically significant wind speed changes occur over ocean areas rather than land areas (Fig. 9a), suggesting less impacts on fire spread and burned area changes. The regions with significantly increased burned areas (Fig. 7a) including boreal forests at high-latitude regions such as Siberia and Canada, rainforests in Southeast Asia, and savannas in Australia show suppressed precipitation in the future, especially rain precipitation (Fig. 9c). In contrast, the tropical regions with decreased burned areas in Fig. 7a also show increasing precipitation tendencies in the future scenario, suggesting strong associations of burning activity with precipitation changes. The relationship between burning activity and temperature changes is less intuitive in most regions except Australia (Fig. 9b), where shows both strong warming tendencies and largely increased burned areas. The complex relations between fire activity and fire weather variables will be discussed further. ¶
The examination of fire, ecosystem, and fire weather variables suggested different feedback mechanisms in these interactions. To quantify different feedback pathways, we compared the sensitivity experiment results with the control runs and isolated atmosphere-centric and vegetation-centric feedback in Fig. 10. The comparison of the fire emission sensitivity experiments (CTRL2-SENS2A) revealed a positive feedback mechanism of fire activity (Fig. 10a) in that fire aerosols tend to suppress precipitation in most regions (Fig. 10b), which agrees well with satellite-based observations (Rosenfeld et al., 2019). It resulted in a 15.7 Mha yr^{-1} increase in global burned area simulations. On the contrary, the comparison of fire-induced land cover change experiments (SENS2A-SENS2B) suggested a negative feedback of fire activity (Fig. 10c) due to reduced fuel load supply (Fig. 10d) in post-fire vegetation changes with consideration of fire-induced LCC. After the incorporation of fire disturbance on land cover, global fuel loads decreased in many post-fire regions such as boreal forest in North America and tropical rainforests and [1]

10a) and increased relative humidity (Fig. 10c), with nonhomogeneous changes of precipitation (Fig. 10b) in response to fire perturbations. These regionally varying results suggest complex interactions between fire and climate systems that merit further investigation.

Therefore, we aggregate regional burned areas in each experiment and compare their changes between the two scenarios to quantify regional effects of different feedback mechanisms (Fig. 11). An atmosphere-centric feedback pathway is identified by comparing relative changes of regional burned area with (i.e., CTRL2-CTRL1) and without (i.e., SENS2A-SENS1A) fire aerosol effects, while a vegetation-centric feedback pathway is identified by comparing relative changes of regional burned area with (i.e., SENS2A-SENS1A) and without (i.e., SENS2B-SENS1B) fire induced LCC. The comparison of relative changes in regional burned area with different feedback pathways reveal distinct regional responses to these fire related atmospheric and vegetation processes. The most significant fire feedback effects occur in North America (Fig. 11a) and South America (Fig. 11b), with the former dominated by negative vegetation-centric fire feedback and the latter dominated by positive atmosphere-centric fire feedback. By including fire induced LCC, the projected burned area increases over North America in the 2050s are greatly suppressed and reduced from +172% in SENS2B to +94% in SENS2A and +93% in CTRL2, respectively. In contrast, the burned area increases over South America considerably enlarges after incorporating fire aerosol effects in the projection, from +112% in SENS2A and +113% in SENS2B to +142% in CTRL2. The fire feedback effects are also evident in many other regions, such as similar positive atmosphere-centric feedbacks in Southeast Asia (Fig. 11g) and Oceania (Fig. 11h) but negative atmosphere-centric feedbacks in Africa (Fig. 11e and 11f). The signs of these feedback effects are determined by fire perturbation on regional fuel and fire weather conditions such as precipitation through fire aerosol-cloud-precipitation interactions or changed vegetation evapotranspiration due to fire induced LCC (Fig. S5 in the Supplement). It's worth noting that these feedback effects could enhance (e.g., North America and Southeast Asia) or compensate (e.g., Northern Hemisphere and Southern Hemisphere Africa) each other in different regions, which further increase the complexity of climate-fire-ecosystem interactions at regional and global scales. On a global average, the net effect of fire feedbacks is almost neutral (Fig. 11i and Table 5) due to the offsetting between positive vegetation-centric and negative atmosphere-centric feedbacks, which are largely dominated by burning activity in African regions.

Lastly, we compare the difference of climate radiative forcing associated with these burning activity changes between the future and present-day scenarios in Table 2 and Fig. 12. Due to broadly increased burning activities in the future projection, fire aerosols are strongly enhanced over most fire-prone regions except Northern Hemisphere Africa and South Asia (Fig. 12a), where the projected burning activity is suppressed as discussed in previous sections. Increased fire aerosols lead to diverse responses in cloud liquid water path, with large increases in high-latitude regions but generally decreases in the tropics and sub-tropics (Fig. 12b). These fire and weather changes result in pronounced responses in radiative forcing through multiple pathways including aerosol-radiation interaction (Fig. 12c), aerosol-cloud interaction (Fig. 12d), and fire induced LCC (Fig. 12e). The fire aerosol related RE changes show more consistent and statistically significant changes over fire-prone regions than these induced by LCC. Previous studies have suggested a net cooling effect of deforestation that could compensate for GHG waring effects on a global scale (Bala et al., 2007;Jin et al., 2012;Randerson et al., 2006). Though our model captures the reduction of forest coverage

and increased springtime albedo in high-latitude regions (Fig. S6 in the Supplement), the radiative effect of fire induced LCC is almost neutral on a global basis in both present-day and future scenarios (Table 2). In general, most burning regions with increased fire aerosols show cooling effects due to enhanced aerosol scattering of solar radiation, while those with decreased fire aerosols show warming effects (Fig. 12c). Fire aerosol direct radiative forcing is overwhelmed by much stronger indirect effects through aerosol-cloud interactions (Fig. 12d), with pervasive cooling effects in high-latitude regions with increased cloudiness (Fig. 12b). Such indirect effects also dominate the net fire radiative effects at both regional and global scales, contributing to a 171% increase of global net fire radiative effect in the RCP4.5 future scenario (Table 2). This projection result is larger than the change in net fire radiative forcing based on the CCSM future projection in Ward et al. (2012), which suggested a 51% increase from -0.55 W m^{-2} in the 2000s to -0.83 W m^{-2} in the 2100s (Table 2). It is noted that their net estimate of fire radiative forcing changes includes other offline-based fire climate effects such as fire-related GHGs impacts and climate-biogeochemical cycle feedbacks, which could dampen the cooling effect of fire aerosols.

3.4 Discussion of modeling uncertainties

As discussed in previous sections, the complex climate-fire-ecosystem interactions in fire related atmospheric and vegetation processes can introduce large uncertainties in the fire projections and associated climate effects. Here we list major uncertainty sources that deserve further investigations in the future.

(1) Future projection of fire triggers such as lightning and human activity is highly uncertain and difficult to explicitly parameterize in global climate models at present. Previous studies suggested different and even contradictory changes in projected lightning in the future (Clark et al., 2017; Finney et al., 2017) due likely to the difference in lightning parameterization schemes used. Pathway dependent long-term projections of demographic data and socioeconomic conditions are also highly uncertain (Riahi et al., 2017). For these reasons, we did not consider these factors in our projection experiments by using fixed demographic and lightning data. Assessing the impacts of these factors will require implementations of different lightning parameterizations and socioeconomic scenarios in climate simulations.

(2) Similar uncertainties arise from future projections of land use and land cover changes and dynamic global vegetation modeling (DGVM). These anthropogenic and ecological processes could directly or indirectly modulate fire activities by changing fire risks and fuel availability. In this study, we used semi-static land use and land cover data with the sole consideration of fire perturbations in both historical and projection scenarios. The inclusion of DGVM will enable the projection of vegetation distributions but introduce additional uncertainties (Zou et al., 2019).

(3) The uncertainties of fire emission estimates arise from those in surface fuel loads, combustion completeness, emission factors, and vertical distributions with rising fire plumes. More measurements of these parameters over extended temporospatial scales are needed to fully evaluate these terms in the fire models. A newly developed fire plume rise scheme (Ke et al., 2019) has been recently implemented in the fire model used in this study and will be used for future fire modeling and evaluation studies.

(4) Last but not the least, fire aerosol radiative effects and aerosol-cloud interactions play an important role in simulating the climate effects of fire aerosols. Though the atmosphere model used in this study incorporates aerosol-cloud interactions, these atmospheric processes across multiple spatial and temporal scales are major contributors to the uncertainties of the climate change assessments (Ciais et al., 2013; Seinfeld et al., 2016). Community wide efforts are ongoing to quantify and reduce the uncertainties of climate modeling discussed above.

4 Conclusions and implications

In this study, we conducted a series of fire-climate modeling experiments for the present-day and future scenarios with explicit implementation of multiple climate-fire-ecosystem feedback mechanisms. We evaluated the CESM-RESFire modeling performance in the context of fire-related radiative effects and terrestrial carbon balance. Various fire radiative effects for the present-day and the RCP4.5 future scenarios are summarized in Fig. 13. We focus on radiative forcing changes related with fire aerosols and fire-induced land cover change. We find an enhanced net fire radiative effect, which is caused by increased global burning activity and subsequent aerosol-cloud interactions, increasing from -0.59 ± 0.51 W m^{-2} in the 2000s to -1.60 ± 0.27 W m^{-2} in the 2050s. Annual global burned area and fire carbon emissions increase by 19% and 100%, respectively, with large amplifications in boreal regions due to suppressed precipitation and enhanced fire ignition and spread rates. These changes imply increasing fire danger over high-latitude regions with prevalent peat lands, which will be more vulnerable to increased fire threats due to climate change. Potential increasing burning activity in these regions may greatly increase fire carbon and tracer gas and aerosol emissions that could have enormous impacts on terrestrial carbon balance and radiative budget. Our modeling results imply that the increase of fire aerosols could compensate the projected decrease of anthropogenic aerosols due to air pollution control policies in many regions (e.g., the eastern U.S. and China) (EPA, 2019;McClure and Jaffe, 2018;Wang et al., 2017;Zhao et al., 2014), where significant aerosol cooling effects dampen GHG warming effects (Goldstein et al., 2009;Rosenfeld et al., 2019). Such counteractive effect to anthropogenic emission reduction would also slow down air quality improvement and reduce associated health benefits revealed by previous studies (Markandya et al., 2018;Zhang et al., 2018).

Fire aerosol emissions and fire-induced land cover change manifest two major feedback mechanisms in climate-fire-ecosystem interactions, showing synergistic or antagonistic effects at regional to global scales. These two distinct feedback mechanisms compete with each other and increase the complexity of interactions among each interactive component. It is noted that we only included the atmosphere and land modeling components of the CESM model to investigate climate effects of global fires with other major components of the earth system including the ocean and sea/land ice in the prescribed data mode. Enhanced climate sensitivity and feedback and uncertainties on a multi-decadal scale might be expected in a fully coupled climate modeling system as previous studies revealed (Dunne et al., 2012;Dunne et al., 2013;Hazeleger et al., 2010;Andrews et al., 2012). We suggest more comprehensive evaluations at regional scales to investigate these complex interactions for major fire-prone regions. More advanced fire modeling capabilities are also needed by integrating additional fire-related processes and climate effects such as fire emitted brown carbon (Brown et al., 2018;Feng et al., 2013;Forrister et al., 2015;Liu et al., 2015;Wang et al., 2018;Zhang et

Deleted: projections
Deleted: simulations
Deleted: We summarized the
Deleted: We mainly considered fire-induced
Deleted: effect
Deleted: found that the
Deleted: was
Deleted: the
Deleted: increased
Deleted: The
Deleted: areas
Deleted: increased
Deleted: at
Deleted: implied
Deleted: dampened
Deleted: opposite
Deleted: a positive atmosphere-centric feedback induced by fire aerosol…
Deleted: and a negative vegetation-centric feedback related with fire-induced land cover and fuel load change.
Deleted: against
Deleted: We also need to advance
Deleted: capability
Deleted: more

al., 2017; Zhang et al., 2019) and fire-vegetation-climate interactions and teleconnections (Garcia et al., 2016;Stark et al., 2016). More evaluation metrics such as large wildfire extreme events should be considered in future studies to improve our understanding of global and regional fire activities, their variations and trends, and their relationship with decadal climate change.

Deleted: activity

Code and data availability

The Level-3 MODIS monthly AOD data from the Aqua platform (MYD08_M3, http://dx.doi.org/10.5067/MODIS/MYD08_M3.006) used for model evaluation are available via NASA Level-1 and Atmosphere Archive & Distribution System (LAADS) Distributed Active Archive Center (DAAC) in https://ladsweb.modaps.eosdis.nasa.gov/missions-and-measurements/products/MYD08_M3/. The AERONET Version 3 Level 2.0 AOT data are available at https://aeronet.gsfc.nasa.gov/. The GFED burned area and fire emission datasets are available at http://www.globalfiredata.org/. All the CESM-RESFire model input and output data reported in the paper are tabulated in the main text and archived on the Cheyenne high-performance computing system (doi:10.5065/D6RX99HX) and High-Performance Storage System (HPSS) managed by the Computational & Information Systems Lab (CISL) of NCAR. The modeling source code and data materials are available upon request, which should be addressed to Yufei Zou (yufei.zou@pnnl.gov).

Deleted: Y. Wang (yuhang.wang@eas.gatech.edu

Author contribution

Y. Zou and Y. Wang designed the experiments and Y. Zou carried them out. Y. Zou developed the model code and performed the simulations. Y. Zou and Y. Wang wrote the manuscript and all co-authors reviewed and edited the manuscript.

Deleted: prepared

Competing interests

The authors declare that they have no conflict of interest.

Acknowledgments

This work was supported by the National Science Foundation (NSF) through grant 1243220 and by the U.S. Department of Energy (DOE)'s office of Science as part of the Regional and Global Climate Modeling Program (NSF-DOE-USDA EaSM2). The Pacific Northwest National Laboratory (PNNL) is operated for DOE by Battelle Memorial Institute under contract DE-AC05-76RL01830. H. Tian was supported by the NSF through grant 1243232. It has not been subjected to any NSF review and therefore does not necessarily reflect the views of the Foundation, and no official endorsement should be inferred.

We would like to acknowledge high-performance computing support from Cheyenne (doi:10.5065/D6RX99HX) provided by NCAR's CISL, sponsored by the National Science Foundation. We are thankful to Steve Platnick for

processing the MODIS AOD data. We thank all the GFED team members for providing the GFED data at http://www.globalfiredata.org/. We thank Wei Min Hao, Brent Holben, Paulo Artaxo, Mikhail Panchenko, Sergey Sakerin, Rachel T. Pinker and their staff for establishing and maintaining the six AERONET sites used in this study. We thank Chandan Sarangi for the helpful discussion to improve the presentation of this work.

References

Abatzoglou, J. T., and Williams, A. P.: Impact of anthropogenic climate change on wildfire across western US forests, P. Natl. Acad. Sci. USA, 113, 11770-11775, 10.1073/pnas.1607171113, 2016.

Abatzoglou, J. T., Williams, A. P., and Barbero, R.: Global Emergence of Anthropogenic Climate Change in Fire Weather Indices, Geophys. Res. Lett., 46, 326-336, 10.1029/2018gl080959, 2019.

Abel, S. J., Highwood, E. J., Haywood, J. M., and Stringer, M. A.: The direct radiative effect of biomass burning aerosols over southern Africa, Atmos. Chem. Phys., 5, 1999-2018, DOI 10.5194/acp-5-1999-2005, 2005.

Albani, S., Mahowald, N.M., Perry, A.T., Scanza, R.A., Zender, C.S., Heavens, N.G., Maggi, V., Kok, J.F. and Otto-Bliesner, B.L.: Improved dust representation in the Community Atmosphere Model. Journal of Advances in Modeling Earth Systems, 6, 541-570, https://doi.org/10.1002/2013MS000279, 2014.

Andela, N., Morton, D. C., Giglio, L., Chen, Y., van der Werf, G. R., Kasibhatla, P. S., DeFries, R. S., Collatz, G. J., Hantson, S., Kloster, S., Bachelet, D., Forrest, M., Lasslop, G., Li, F., Mangeon, S., Melton, J. R., Yue, C., Randerson, J. T.: A human-driven decline in global burned area, Science, 356(6345), 1356–1362. https://doi.org/10.1126/science.aal4108, 2017.

Andela, N., and van der Werf, G. R.: Recent trends in African fires driven by cropland expansion and El Nino to La Nina transition, Nature Climate Change, 4, 791–795. https://doi.org/10.1038/nclimate2313, 2014.

Andrews, T., Gregory, J. M., Webb, M. J., and Taylor, K. E.: Forcing, feedbacks and climate sensitivity in CMIP5 coupled atmosphere-ocean climate models, Geophys. Res. Lett., 39, Artn L0971210.1029/2012gl051607, 2012.

Bala, G., Caldeira, K., Wickett, M., Phillips, T. J., Lobell, D. B., Delire, C., and Mirin, A.: Combined climate and carbon-cycle effects of large-scale deforestation, P. Natl. Acad. Sci. USA, 104, 6550-6555, 10.1073/pnas.0608998104, 2007.

Barbero, R., Abatzoglou, J. T., Larkin, N. K., Kolden, C. A., and Stocks, B.: Climate change presents increased potential for very large fires in the contiguous United States, Int. J. Wildland Fire, 24, 892-899, 10.1071/Wf15083, 2015.

Bowman, D. M. J. S., Balch, J. K., Artaxo, P., Bond, W. J., Carlson, J. M., Cochrane, M. A., D'Antonio, C. M., DeFries, R. S., Doyle, J. C., Harrison, S. P., Johnston, F. H., Keeley, J. E., Krawchuk, M. A., Kull, C. A., Marston, J. B., Moritz, M. A., Prentice, I. C., Roos, C. I., Scott, A. C., Swetnam, T. W., van der Werf, G. R., and Pyne, S. J.: Fire in the Earth System, Science, 324, 481-484, 10.1126/science.1163886, 2009.

Brown, H., Liu, X. H., Feng, Y., Jiang, Y. Q., Wu, M. X., Lu, Z., Wu, C. L., Murphy, S., and Pokhrel, R.: Radiative effect and climate impacts of brown carbon with the Community Atmosphere Model (CAM5), Atmos. Chem. Phys., 18, 17745-17768, 10.5194/acp-18-17745-2018, 2018.

Ciais, P., C. Sabine, G. Bala, L. Bopp, V. Brovkin, J. Canadell, A. Chhabra, R. DeFries, J. Galloway, M. Heimann, C. Jones, C. Le Quéré, R.B. Myneni, and Thornton, S. P. a. P.: Carbon and Other Biogeochemical Cycles in Climate Change 2013: The Physical Science Basis, Cambridge, United Kingdom and New York, NY, USA, 2013.

Clarke, H., Lucas, C., and Smith, P.: Changes in Australian fire weather between 1973 and 2010, Int. J. Climatol., 33, 931-944, 10.1002/joc.3480, 2013.

Clark, S. K., Ward, D. S., and Mahowald, N. M.: Parameterization-based uncertainty in future lightning flash density, Geophys. Res. Lett., 44, 2893–2901, doi:10.1002/2017GL073017, 2017.

Computational and Information Systems Laboratory (CISL). Cheyenne: HPE/SGI ICE XA System (University Community Computing). Boulder, CO: National Center for Atmospheric Research. doi:10.5065/D6RX99HX, 2017.

Dennison, P. E., Brewer, S. C., Arnold, J. D., and Moritz, M. A.: Large wildfire trends in the western United States, 1984-2011, Geophys. Res. Lett., 41, 2928-2933, 10.1002/2014gl059576, 2014.

Dentener, F., Kinne, S., Bond, T., Boucher, O., Cofala, J., Generoso, S., Ginoux, P., Gong, S., Hoelzemann, J. J., Ito, A., Marelli, L., Penner, J. E., Putaud, J. P., Textor, C., Schulz, M., van der Werf, G. R., and Wilson, J.: Emissions of primary aerosol and precursor gases in the years 2000 and 1750 prescribed data-sets for AeroCom, Atmos. Chem. Phys., 6, 4321-4344, DOI 10.5194/acp-6-4321-2006, 2006.

Dunne, J. P., John, J. G., Adcroft, A. J., Griffies, S. M., Hallberg, R. W., Shevliakova, E., Stouffer, R. J., Cooke, W., Dunne, K. A., Harrison, M. J., Krasting, J. P., Malyshev, S. L., Milly, P. C. D., Phillipps, P. J., Sentman, L. T., Samuels, B. L., Spelman, M. J., Winton, M., Wittenberg, A. T., and Zadeh, N.: GFDL's ESM2 Global Coupled Climate-Carbon Earth System Models. Part I: Physical Formulation and Baseline Simulation Characteristics, J. Climate, 25, 6646-6665, 10.1175/Jcli-D-11-00560.1, 2012.

Dunne, J. P., John, J. G., Shevliakova, E., Stouffer, R. J., Krasting, J. P., Malyshev, S. L., Milly, P. C. D., Sentman, L. T., Adcroft, A. J., Cooke, W., Dunne, K. A., Griffies, S. M., Hallberg, R. W., Harrison, M. J., Levy, H., Wittenberg, A. T., Phillips, P. J., and Zadeh, N.: GFDL's ESM2 Global Coupled Climate-Carbon Earth System Models. Part II: Carbon System Formulation and Baseline Simulation Characteristics, J. Climate, 26, 2247-2267, 10.1175/Jcli-D-12-00150.1, 2013.

Particulate Matter (PM2.5) trends: https://www.epa.gov/air-trends/particulate-matter-pm25-trends, access: Feburary 19, 2019.

Fann, N., Alman, B., Broome, R. A., Morgan, G. G., Johnston, F. H., Pouliot, G., and Rappold, A. G.: The health impacts and economic value of wildland fire episodes in the US: 2008-2012, Sci. Total. Environ., 610, 802-809, 10.1016/j.scitotenv.2017.08.024, 2018.

Feng, Y., Ramanathan, V., and Kotamarthi, V. R.: Brown carbon: a significant atmospheric absorber of solar radiation?, Atmos. Chem. Phys., 13, 8607-8621, 10.5194/acp-13-8607-2013, 2013.

Finney, D.L., Doherty, R.M., Wild, O., Stevenson, D.S., MacKenzie, I.A. and Blyth, A.M.: A projected decrease in lightning under climate change. Nat. Clim. Change, 8, 210, https://doi.org/10.1038/s41558-018-0072-6, 2018.

Flanner, M. G., and Zender, C. S.: Snowpack radiative heating: Influence on Tibetan Plateau climate, Geophys. Res. Lett., 32, Artn L0650110.1029/2004gl022076, 2005.

Flannigan, M., Cantin, A. S., de Groot, W. J., Wotton, M., Newbery, A., and Gowman, L. M.: Global wildland fire season severity in the 21st century, Forest Ecol. Manag., 294, 54-61, 10.1016/j.foreco.2012.10.022, 2013.

Flannigan, M. D., Krawchuk, M. A., de Groot, W. J., Wotton, B. M., and Gowman, L. M.: Implications of changing climate for global wildland fire, Int. J. Wildland Fire, 18, 483-507, 10.1071/Wf08187, 2009.

Forrister, H., Liu, J., Scheuer, E., Dibb, J., Ziemba, L., Thornhill, K. L., Anderson, B., Diskin, G., Perring, A. E., Schwarz, J. P., Campuzano-Jost, P., Day, D. A., Palm, B. B., Jimenez, J. L., Nenes, A., and Weber, R. J.: Evolution of brown carbon in wildfire plumes, Geophys. Res. Lett., 42, 4623-4630, 10.1002/2015gl063897, 2015.

Garcia, E. S., Swann, A. L. S., Villegas, J. C., Breshears, D. D., Law, D. J., Saleska, S. R., and Stark, S. C.: Synergistic Ecoclimate Teleconnections from Forest Loss in Different Regions Structure Global Ecological Responses, Plos One, 11, ARTN e016504210.1371/journal.pone.0165042, 2016.

Ghan, S. J.: Technical Note: Estimating aerosol effects on cloud radiative forcing, Atmos. Chem. Phys., 13, 9971-9974, 10.5194/acp-13-9971-2013, 2013.

Giglio, L., Randerson, J. T., and van der Werf, G. R.: Analysis of daily, monthly, and annual burned area using the fourth-generation global fire emissions database (GFED4), J. Geophys. Res.-Biogeo., 118, 317-328, 10.1002/jgrg.20042, 2013.

Gilardoni, S., Vignati, E., Marmer, E., Cavalli, F., Belis, C., Gianelle, V., Loureiro, A., and Artaxo, P.: Sources of carbonaceous aerosol in the Amazon basin, Atmos. Chem. Phys., 11, 2747-2764, 10.5194/acp-11-2747-2011, 2011.

Goldstein, A. H., Koven, C. D., Heald, C. L., and Fung, I. Y.: Biogenic carbon and anthropogenic pollutants combine to form a cooling haze over the southeastern United States, P. Natl. Acad. Sci. USA, 106, 8835-8840, 10.1073/pnas.0904128106, 2009.

Hall, J. R.: The total cost of fire in the United States, National Fire Protection Association, Quincy, MA, 38, 2014.

Hantson, S., Arneth, A., Harrison, S. P., Kelley, D. I., Prentice, I. C., Rabin, S. S., Archibald, S., Mouillot, F., Arnold, S. R., Artaxo, P., Bachelet, D., Ciais, P., Forrest, M., Friedlingstein, P., Hickler, T., Kaplan, J. O., Kloster, S., Knorr, W., Lasslop, G., Li, F., Mangeon, S., Melton, J. R., Meyn, A., Sitch, S., Spessa, A., van der Werf, G. R., Voulgarakis, A., and Yue, C.: The status and challenge of global fire modelling, Biogeosciences, 13, 3359-3375, 10.5194/bg-13-3359-2016, 2016.

Harris, R. M. B., Remenyi, T. A., Williamson, G. J., Bindoff, N. L., and Bowman, D. M. J. S.: Climate-vegetation-fire interactions and feedbacks: trivial detail or major barrier to projecting the future of the Earth system?, Wires Clim. Change, 7, 910-931, 10.1002/wcc.428, 2016.

Hazeleger, W., Severijns, C., Semmler, T., Stefanescu, S., Yang, S. T., Wang, X. L., Wyser, K., Dutra, E., Baldasano, J. M., Bintanja, R., Bougeault, P., Caballero, R., Ekman, A. M. L., Christensen, J. H., van den Hurk, B., Jimenez, P., Jones, C., Kallberg, P., Koenigk, T., McGrath, R., Miranda, P., Van Noije, T., Palmer, T., Parodi, J. A., Schmith, T., Selten, F., Storelvmo, T., Sterl, A., Tapamo, H., Vancoppenolle, M., Viterbo, P., and Willen, U.: EC-Earth A Seamless Earth-System Prediction Approach in Action, B. Am. Meteorol. Soc., 91, 1357-1363, 10.1175/2010bams2877.1, 2010.

Horowitz, L.W., Walters, S., Mauzerall, D.L., Emmons, L.K., Rasch, P.J., Granier, C., Tie, X., Lamarque, J.F., Schultz, M.G., Tyndall, G.S. and Orlando, J.J.: A global simulation of tropospheric ozone and related tracers: Description and evaluation of MOZART, version 2. J. Geophys. Res.-Atmos., 108, 2003.

Hurrell, J. W., Holland, M. M., Gent, P. R., Ghan, S., Kay, J. E., Kushner, P. J., Lamarque, J. F., Large, W. G., Lawrence, D., Lindsay, K., Lipscomb, W. H., Long, M. C., Mahowald, N., Marsh, D. R., Neale, R. B., Rasch, P., Vavrus, S., Vertenstein, M., Bader, D., Collins, W. D., Hack, J. J., Kiehl, J., and Marshall, S.: The Community Earth System Model A Framework for Collaborative Research, B. Am. Meteorol. Soc., 94, 1339-1360, 10.1175/Bams-D-12-00121.1, 2013.

Hurteau, M. D., Westerling, A. L., Wiedinmyer, C., and Bryant, B. P.: Projected Effects of Climate and Development on California Wildfire Emissions through 2100, Environ. Sci. Technol., 48, 2298-2304, 10.1021/es4050133, 2014.

Hurtt, G. C., Frolking, S., Fearon, M. G., Moore, B., Shevliakova, E., Malyshev, S., Pacala, S. W., and Houghton, R. A.: The underpinnings of land-use history: three centuries of global gridded land-use transitions, wood-harvest activity, and resulting secondary lands, Global Change Biol., 12, 1208-1229, 10.1111/j.1365-2486.2006.01150.x, 2006.

Jiang, Y. Q., Lu, Z., Liu, X. H., Qian, Y., Zhang, K., Wang, Y. H., and Yang, X. Q.: Impacts of global open-fire aerosols on direct radiative, cloud and surface-albedo effects simulated with CAM5, Atmos. Chem. Phys., 16, 14805-14824, 10.5194/acp-16-14805-2016, 2016.

Jin, Y. F., Randerson, J. T., Goetz, S. J., Beck, P. S. A., Loranty, M. M., and Goulden, M. L.: The influence of burn severity on postfire vegetation recovery and albedo change during early succession in North American boreal forests, J. Geophys. Res.-Biogeo., 117, Artn G0103610.1029/2011jg001886, 2012.

Johnston, F. H., Henderson, S. B., Chen, Y., Randerson, J. T., Marlier, M., DeFries, R. S., Kinney, P., Bowman, D. M. J. S., and Brauer, M.: Estimated Global Mortality Attributable to Smoke from Landscape Fires, Environ. Health Persp., 120, 695-701, 10.1289/ehp.1104422, 2012.

Jolly, W. M., Cochrane, M. A., Freeborn, P. H., Holden, Z. A., Brown, T. J., Williamson, G. J., and Bowman, D. M. J. S.: Climate-induced variations in global wildfire danger from 1979 to 2013, Nat. Commun., 6, ARTN 753710.1038/ncomms8537, 2015.

Ke, Z., Wang, Y., Zou, Y., Song, Y., and Liu, Y.: The global plume-rise dataset and its climate model implement, submitted to J. Adv. Model Earth Sy., 2019.

Kloster, S., Mahowald, N. M., Randerson, J. T., Thornton, P. E., Hoffman, F. M., Levis, S., Lawrence, P. J., Feddema, J. J., Oleson, K. W., and Lawrence, D. M.: Fire dynamics during the 20th century simulated by the Community Land Model, Biogeosciences, 7, 1877-1902, 10.5194/bg-7-1877-2010, 2010.

Kloster, S., Mahowald, N. M., Randerson, J. T., and Lawrence, P. J.: The impacts of climate, land use, and demography on fires during the 21st century simulated by CLM-CN, Biogeosciences, 9, 509-525, 10.5194/bg-9-509-2012, 2012.

Kurokawa, J., Ohara, T., Morikawa, T., Hanayama, S., Janssens-Maenhout, G., Fukui, T., Kawashima, K., and Akimoto, H.: Emissions of air pollutants and greenhouse gases over Asian regions during 2000-2008: Regional

Emission inventory in ASia (REAS) version 2, Atmos. Chem. Phys., 13, 11019-11058, 10.5194/acp-13-11019-2013, 2013.

Lamarque, J. F., Bond, T. C., Eyring, V., Granier, C., Heil, A., Klimont, Z., Lee, D., Liousse, C., Mieville, A., Owen, B., Schultz, M. G., Shindell, D., Smith, S. J., Stehfest, E., Van Aardenne, J., Cooper, O. R., Kainuma, M., Mahowald, N., McConnell, J. R., Naik, V., Riahi, K., and van Vuuren, D. P.: Historical (1850-2000) gridded anthropogenic and biomass burning emissions of reactive gases and aerosols: methodology and application, Atmos. Chem. Phys., 10, 7017-7039, 10.5194/acp-10-7017-2010, 2010.

Le Quere, C., Andres, R. J., Boden, T., Conway, T., Houghton, R. A., House, J. I., Marland, G., Peters, G. P., van der Werf, G. R., Ahlstrom, A., Andrew, R. M., Bopp, L., Canadell, J. G., Ciais, P., Doney, S. C., Enright, C., Friedlingstein, P., Huntingford, C., Jain, A. K., Jourdain, C., Kato, E., Keeling, R. F., Goldewijk, K. K., Levis, S., Levy, P., Lomas, M., Poulter, B., Raupach, M. R., Schwinger, J., Sitch, S., Stocker, B. D., Viovy, N., Zaehle, S., and Zeng, N.: The global carbon budget 1959-2011, Earth Syst. Sci. Data, 5, 165-185, 10.5194/essd-5-165-2013, 2013.

Li, F., Levis, S., and Ward, D. S.: Quantifying the role of fire in the Earth system - Part 1: Improved global fire modeling in the Community Earth System Model (CESM1), Biogeosciences, 10, 2293-2314, 10.5194/bg-10-2293-2013, 2013.

Li, F., Bond-Lamberty, B., and Levis, S.: Quantifying the role of fire in the Earth system - Part 2: Impact on the net carbon balance of global terrestrial ecosystems for the 20th century, Biogeosciences, 11, 1345-1360, 10.5194/bg-11-1345-2014, 2014.

Liu, J., Scheuer, E., Dibb, J., Diskin, G. S., Ziemba, L. D., Thornhill, K. L., Anderson, B. E., Wisthaler, A., Mikoviny, T., Devi, J. J., Bergin, M., Perring, A. E., Markovic, M. Z., Schwarz, J. P., Campuzano-Jost, P., Day, D. A., Jimenez, J. L., and Weber, R. J.: Brown carbon aerosol in the North American continental troposphere: sources, abundance, and radiative forcing, Atmos. Chem. Phys., 15, 7841-7858, 10.5194/acp-15-7841-2015, 2015.

Liu, X., Easter, R. C., Ghan, S. J., Zaveri, R., Rasch, P., Shi, X., Lamarque, J. F., Gettelman, A., Morrison, H., Vitt, F., Conley, A., Park, S., Neale, R., Hannay, C., Ekman, A. M. L., Hess, P., Mahowald, N., Collins, W., Iacono, M. J., Bretherton, C. S., Flanner, M. G., and Mitchell, D.: Toward a minimal representation of aerosols in climate models: description and evaluation in the Community Atmosphere Model CAM5, Geosci. Model Dev., 5, 709-739, 10.5194/gmd-5-709-2012, 2012.

Liu, Y., Zhang, K., Qian, Y., Wang, Y., Zou, Y., Song, Y., Wan, H., Liu, X., and Yang, X.-Q.: Investigation of short-term effective radiative forcing of fire aerosols over North America using nudged hindcast ensembles, Atmos. Chem. Phys., 18, 31-47, 10.5194/acp-18-31-2018, 2018.

Liu, Y. Q.: New development and application needs for Earth system modeling of fire-climate-ecosystem interactions, Environ. Res. Lett., 13, ARTN 01100110.1088/1748-9326/aaa347, 2018.

Liu, Y. Q., Stanturf, J., and Goodrick, S.: Trends in global wildfire potential in a changing climate, Forest Ecol. Manag., 259, 685-697, 10.1016/j.foreco.2009.09.002, 2010.

Lu, Z., Liu, X., Zhang, Z., Zhao, C., Meyer, K., Rajapakshe, C., Wu, C., Yang, Z. and Penner, J.E.: Biomass smoke from southern Africa can significantly enhance the brightness of stratocumulus over the southeastern Atlantic Ocean. Proc. Natl. Acad. Sci. U.S.A., 115, 2924-2929, https://doi.org/10.1073/pnas.1713703115, 2018.

Markandya, A., Sampedro, J., Smith, S. J., Dingenen, R. V., Pizarro-Irizar, C., Arto, I., and González-Eguino, M.: Health co-benefits from air pollution and mitigation costs of the Paris Agreement: a modelling study, The Lancet Planetary Health, 2, e126-e133, https://doi.org/10.1016/S2542-5196(18)30029-9, 2018.

Martin, M. V., Logan, J. A., Kahn, R. A., Leung, F. Y., Nelson, D. L., and Diner, D. J.: Smoke injection heights from fires in North America: analysis of 5 years of satellite observations, Atmos. Chem. Phys., 10, 1491-1510, 2010.

McClure, C. D., and Jaffe, D. A.: US particulate matter air quality improves except in wildfire-prone areas, P. Natl. Acad. Sci. USA, 115, 7901-7906, 10.1073/pnas.1804353115, 2018.

Moritz, M. A., Parisien, M. A., Batllori, E., Krawchuk, M. A., Van Dorn, J., Ganz, D. J., and Hayhoe, K.: Climate change and disruptions to global fire activity, Ecosphere, 3, Unsp 4910.1890/Es11-00345.1, 2012.

Neale, R. B., Chen, C. C., Gettelman, A., Lauritzen, P. H., Park, S., Williamson, D. L., Conley, A. J., Garcia, R., Kinnison, D., Lamarque, J. F., Marsh, D., Mills, M., Smith, A. K., Tilmes, S., Vitt, F., Morrison, H., Cameron-Smith, P., Collins, W. D., Iacono, M. J., Easter, R. C., Ghan, S. J., Liu, X. H., Rasch, P. J., and Taylor, M. A.: Description of the NCAR Community Atmosphere Model (CAM 5.0), NCAR 289, 2013.

Oleson, K. W., Lawrence, D. M., Bonan, G. B., Drewniak, B., Huang, M., Koven, C. D., Levis, S., Li, F., Riley, W. J., Subin, Z. M., Swenson, S. C., Thornton, P. E., Bozbiyik, A., Fisher, R., Heald, C. L., Kluzek, E., Lamarque, J.-F., Lawrence, P. J., Leung, L. R., Lipscomb, W., Muszala, S., Ricciuto, D. M., Sacks, W., Sun, Y., Tang, J., and Yang, Z.-L.: Technical description of version 4.5 of the Community Land Model (CLM), NCAR 434, 2013.

Park, S., Bretherton, C. S., and Rasch, P. J.: Integrating Cloud Processes in the Community Atmosphere Model, Version 5, J. Climate, 27, 6821-6856, 10.1175/Jcli-D-14-00087.1, 2014.

Parks, S. A., Miller, C., Abatzoglou, J. T., Holsinger, L. M., Parisien, M. A., and Dobrowski, S. Z.: How will climate change affect wildland fire severity in the western US?, Environ. Res. Lett., 11, Artn 03500210.1088/1748-9326/11/3/035002, 2016.

Pellegrini, A. F. A., Ahlstrom, A., Hobbie, S. E., Reich, P. B., Nieradzik, L. P., Staver, A. C., Scharenbroch, B. C., Jumpponen, A., Anderegg, W. R. L., Randerson, J. T., and Jackson, R. B.: Fire frequency drives decadal changes in soil carbon and nitrogen and ecosystem productivity, Nature, 553, 194-198, 10.1038/nature24668, 2018.

Piao, S. L., Sitch, S., Ciais, P., Friedlingstein, P., Peylin, P., Wang, X. H., Ahlstrom, A., Anav, A., Canadell, J. G., Cong, N., Huntingford, C., Jung, M., Levis, S., Levy, P. E., Li, J. S., Lin, X., Lomas, M. R., Lu, M., Luo, Y. Q., Ma, Y. C., Myneni, R. B., Poulter, B., Sun, Z. Z., Wang, T., Viovy, N., Zaehle, S., and Zeng, N.: Evaluation of terrestrial carbon cycle models for their response to climate variability and to CO2 trends, Global Change Biol., 19, 2117-2132, 10.1111/gcb.12187, 2013.

Quillet, A., Peng, C, Garneau, M.: Toward dynamic global vegetation models for simulating vegetation–climate interactions and feedbacks: recent developments, limitations, and future challenges, Environmental Reviews, 18(NA), 333-53, 10.1139/A10-016, 2010.

Randerson, J. T., Liu, H., Flanner, M. G., Chambers, S. D., Jin, Y., Hess, P. G., Pfister, G., Mack, M. C., Treseder, K. K., Welp, L. R., Chapin, F. S., Harden, J. W., Goulden, M. L., Lyons, E., Neff, J. C., Schuur, E. A. G., and Zender, C. S.: The impact of boreal forest fire on climate warming, Science, 314, 1130-1132, 10.1126/science.1132075, 2006.

Randerson, J. T., Chen, Y., van der Werf, G. R., Rogers, B. M., and Morton, D. C.: Global burned area and biomass burning emissions from small fires, J. Geophys. Res.-Biogeo., 117, Artn G0401210.1029/2012jg002128, 2012.

Rayner, N. A., Parker, D. E., Horton, E. B., Folland, C. K., Alexander, L. V., Rowell, D. P., Kent, E. C., and Kaplan, A.: Global analyses of sea surface temperature, sea ice, and night marine air temperature since the late nineteenth century, J. Geophys. Res.-Atmos., 108, Artn 440710.1029/2002jd002670, 2003.

Riahi, K., Van Vuuren, D.P., Kriegler, E., Edmonds, J., O'neill, B.C., Fujimori, S., Bauer, N., Calvin, K., Dellink, R., Fricko, O. and Lutz, W.: The shared socioeconomic pathways and their energy, land use, and greenhouse gas emissions implications: an overview. Global Environmental Change, 42, 153-168, http://dx.doi.org/10.1016/j.gloenvcha.2016.05.009, 2017.

Platnick, S., Hubanks, P., Meyer, K., and King, M. D.: MODIS Atmosphere L3 Monthly Product. NASA MODIS Adaptive Processing System, Goddard Space Flight Center, USA: http://dx.doi.org/10.5067/MODIS/MYD08_M3.061, 2015.

Richardson, L. A., Champ, P. A., and Loomis, J. B.: The hidden cost of wildfires: Economic valuation of health effects of wildfire smoke exposure in Southern California, J. Forest. Econ., 18, 14-35, 10.1016/j.jfe.2011.05.002, 2012.

Rosenfeld, D., Zhu, Y. N., Wang, M. H., Zheng, Y. T., Goren, T., and Yu, S. C.: Aerosol-driven droplet concentrations dominate coverage and water of oceanic low-level clouds, Science, 363, 599-+, ARTN eaav056610.1126/science.aav0566, 2019.

Seidl, R., Thom, D., Kautz, M., Martin-Benito, D., Peltoniemi, M., Vacchiano, G., Wild, J., Ascoli, D., Petr, M., Honkaniemi, J., Lexer, M. J., Trotsiuk, V., Mairota, P., Svoboda, M., Fabrika, M., Nagel, T. A., and Reyer, C. P. O.: Forest disturbances under climate change, Nat. Clim. Change, 7, 395-402, 10.1038/Nclimate3303, 2017.

Seinfeld, J.H., Bretherton, C., Carslaw, K.S., Coe, H., DeMott, P.J., Dunlea, E.J., Feingold, G., Ghan, S., Guenther, A.B., Kahn, R. and Kraucunas, I.: Improving our fundamental understanding of the role of aerosol−cloud interactions in the climate system. Proc. Natl. Acad. Sci. U.S.A., 113, 5781-5790, 2016.

Seo, H., and Kim, Y.: Interactive impacts of fire and vegetation dynamics on global carbon and water budget using Community Land Model version 4.5, Geosci. Model. Dev., 12, 457-472, 10.5194/gmd-12-457-2019, 2019.

Shuman, J. K., Foster, A. C., Shugart, H. H., Hoffman-Hall, A., Krylov, A., Loboda, T., Ershov, D., and Sochilova, E.: Fire disturbance and climate change: implications for Russian forests, Environ. Res. Lett., 12, ARTN 03500310.1088/1748-9326/aa5eed, 2017.

Sofiev, M., Ermakova, T., and Vankevich, R.: Evaluation of the smoke-injection height from wild-land fires using remote-sensing data, Atmos. Chem. Phys., 12, 1995-2006, 10.5194/acp-12-1995-2012, 2012.

Stark, S. C., Breshears, D. D., Garcia, E. S., Law, D. J., Minor, D. M., Saleska, S. R., Swann, A. L. S., Villegas, J. C., Aragao, L. E. O. C., Bella, E. M., Borma, L. S., Cobb, N. S., Litvak, M. E., Magnusson, W. E., Morton, J. M., and

Deleted: Ridley, D. A., Heald, C. L., Kok, J. F., and Zhao, C.: An observationally constrained estimate of global dust aerosol optical depth, Atmos.

Moved down [2]: Chem.

Deleted: Phys., 16, 15097-15117, 10.5194/acp-16-15097-2016, 2016.¶

Redmond, M. D.: Toward accounting for ecoclimate teleconnections: intra- and inter-continental consequences of altered energy balance after vegetation change, Landscape Ecol., 31, 181-194, 10.1007/s10980-015-0282-5, 2016.

Sun, Y., Gu, L. H., and Dickinson, R. E.: A numerical issue in calculating the coupled carbon and water fluxes in a climate model, J. Geophys. Res.-Atmos., 117, Artn D2210310.1029/2012jd018059, 2012.

Thomas, D., Butry, D., Gilbert, S., Webb, D., and Fung, J.: The costs and losses of wildfires: A literature review, National Institute of Standards and Technology, 72, 2017.

Thonicke, K., Spessa, A., Prentice, I. C., Harrison, S. P., Dong, L., and Carmona-Moreno, C.: The influence of vegetation, fire spread and fire behaviour on biomass burning and trace gas emissions: results from a process-based model, Biogeosciences, 7, 1991-2011, 10.5194/bg-7-1991-2010, 2010.

Tosca, M. G., Randerson, J. T., and Zender, C. S.: Global impact of smoke aerosols from landscape fires on climate and the Hadley circulation, Atmos. Chem. Phys., 13, 5227-5241, 10.5194/acp-13-5227-2013, 2013.

Tost, H., Jöckel, P., and Lelieveld, J.: Lightning and convection parameterisations – uncertainties in global modelling, Atmos. Chem. Phys., 7, 4553–4568, https://doi.org/10.5194/acp-7-4553-2007, 2007.

van der Werf, G. R., Randerson, J. T., Giglio, L., Collatz, G. J., Kasibhatla, P. S., and Arellano, A. F.: Interannual variability in global biomass burning emissions from 1997 to 2004, Atmos. Chem. Phys., 6, 3423-3441, DOI 10.5194/acp-6-3423-2006, 2006.

van der Werf, G. R., Randerson, J. T., Giglio, L., van Leeuwen, T. T., Chen, Y., Rogers, B. M., Mu, M. Q., van Marle, M. J. E., Morton, D. C., Collatz, G. J., Yokelson, R. J., and Kasibhatla, P. S.: Global fire emissions estimates during 1997-2016, Earth Syst. Sci. Data, 9, 697-720, 10.5194/essd-9-697-2017, 2017.

Wang, J. D., Zhao, B., Wang, S. X., Yang, F. M., Xing, J., Morawska, L., Ding, A. J., Kulmala, M., Kerminen, V. M., Kujansuu, J., Wang, Z. F., Ding, D. A., Zhang, X. Y., Wang, H. B., Tian, M., Petaja, T., Jiang, J. K., and Hao, J. M.: Particulate matter pollution over China and the effects of control policies, Sci. Total Environ., 584, 426-447, 10.1016/j.scitotenv.2017.01.027, 2017.

Wang, X., Heald, C. L., Liu, J. M., Weber, R. J., Campuzano-Jost, P., Jimenez, J. L., Schwarz, J. P., and Perring, A. E.: Exploring the observational constraints on the simulation of brown carbon, Atmos. Chem. Phys., 18, 635-653, 10.5194/acp-18-635-2018, 2018.

Ward, D. S., Kloster, S., Mahowald, N. M., Rogers, B. M., Randerson, J. T., and Hess, P. G.: The changing radiative forcing of fires: global model estimates for past, present and future, Atmos. Chem. Phys., 12, 10857-10886, 10.5194/acp-12-10857-2012, 2012.

Westerling, A. L., Hidalgo, H. G., Cayan, D. R., and Swetnam, T. W.: Warming and earlier spring increase western US forest wildfire activity, Science, 313, 940-943, 10.1126/science.1128834, 2006.

Wotton, B. M., Flannigan, M. D., and Marshall, G. A.: Potential climate change impacts on fire intensity and key wildfire suppression thresholds in Canada, Environ. Res. Lett., 12, ARTN 09500310.1088/1748-9326/aa7e6e, 2017.

Yang, G., Di, X. Y., Guo, Q. X., Shu, Z., Zeng, T., Yu, H. Z., and Wang, C.: The impact of climate change on forest fire danger rating in China's boreal forest, J. For. Res., 22, 249-257, 10.1007/s11676-011-0158-8, 2011.

Moved (insertion) [2]

Yang, J., Tian, H. Q., Tao, B., Ren, W., Pan, S. F., Liu, Y. Q., and Wang, Y. H.: A growing importance of large fires in conterminous United States during 1984-2012, J. Geophys. Res.-Biogeo., 120, 2625-2640, 10.1002/2015jg002965, 2015.

Young, A. M., Higuera, P. E., Duffy, P. A., and Hu, F. S.: Climatic thresholds shape northern high-latitude fire regimes and imply vulnerability to future climate change, Ecography., 40, 606-617, 10.1111/ecog.02205, 2017.

Yue, C., Ciais, P., Cadule, P., Thonicke, K., and van Leeuwen, T. T.: Modelling the role of fires in the terrestrial carbon balance by incorporating SPITFIRE into the global vegetation model ORCHIDEE - Part 2: Carbon emissions and the role of fires in the global carbon balance, Geosci. Model Dev., 8, 1321-1338, 10.5194/gmd-8-1321-2015, 2015.

Yue, C., Ciais, P., Zhu, D., Wang, T., Peng, S. S., and Piao, S. L.: How have past fire disturbances contributed to the current carbon balance of boreal ecosystems?, Biogeosciences, 13, 675-690, 10.5194/bg-13-675-2016, 2016.

Yue, X., Mickley, L. J., Logan, J. A., and Kaplan, J. O.: Ensemble projections of wildfire activity and carbonaceous aerosol concentrations over the western United States in the mid-21st century, Atmos. Environ., 77, 767-780, 10.1016/j.atmosenv.2013.06.003, 2013.

Zhang, A., Wang, Y., Zhang, Y., Weber, R. J., Song, Y., Ke, Z., and Zou, Y.: Modeling global radiative effect of brown carbon: A larger heating source in the tropical free troposphere than black carbon, Atmos. Chem. Phys. Discuss., https://doi.org/10.5194/acp-2019-594, in review, 2019.

Zhang, Y., West, J. J., Mathur, R., Xing, J., Hogrefe, C., Roselle, S. J., Bash, J. O., Pleim, J. E., Gan, C.-M., and Wong, D. C.: Long-term trends in the ambient $PM_{2.5}$- and O_3-related mortality burdens in the United States under emission reductions from 1990 to 2010, Atmos. Chem. Phys., 18, 15003-15016, https://doi.org/10.5194/acp-18-15003-2018, 2018.

Zhang, Y. Z., Forrister, H., Liu, J. M., Dibb, J., Anderson, B., Schwarz, J. P., Perring, A. E., Jimenez, J. L., Campuzano-Jost, P., Wang, Y. H., Nenes, A., and Weber, R. J.: Top-of-atmosphere radiative forcing affected by brown carbon in the upper troposphere, Nat. Geosci., 10, 486-+, 10.1038/Ngeo2960, 2017.

Zhang, Z., Meyer, K., Yu, H., Platnick, S., Colarco, P., Liu, Z., and Oreopoulos, L.: Shortwave direct radiative effects of above-cloud aerosols over global oceans derived from 8 years of CALIOP and MODIS observations, Atmos. Chem. Phys., 16, 2877-2900, 10.5194/acp-16-2877-2016, 2016.

Zhao, M. S., Heinsch, F. A., Nemani, R. R., and Running, S. W.: Improvements of the MODIS terrestrial gross and net primary production global data set, Remote Sens. Environ., 95, 164-176, 10.1016/j.rse.2004.12.011, 2005.

Zhao, M. S., and Running, S. W.: Drought-Induced Reduction in Global Terrestrial Net Primary Production from 2000 Through 2009, Science, 329, 940-943, 10.1126/science.1192666, 2010.

Zhao, Y., Zhang, J., and Nielsen, C. P.: The effects of energy paths and emission controls and standards on future trends in China's emissions of primary air pollutants, Atmos. Chem. Phys., 14, 8849-8868, 10.5194/acp-14-8849-2014, 2014.

Zou, Y., Wang, Y., Ke, Z., Tian, H., Yang, J., and Liu, Y.: Development of a REgion-Specific ecosystem feedback Fire (RESFire) model in the Community Earth System Model, J. Adv. Model Earth Sy., https://doi.org/10.1029/2018MS001368, 2019.

Deleted: .

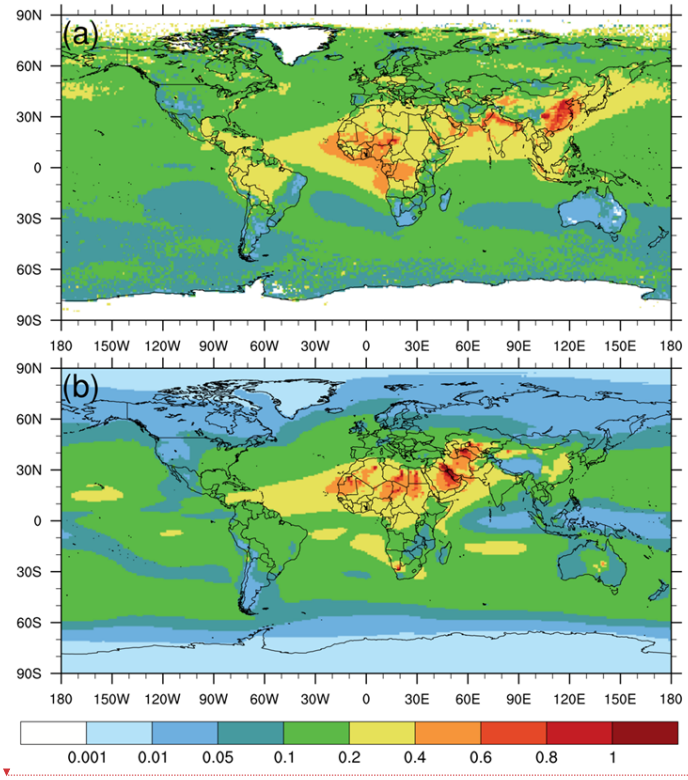

Figure 1: Comparison of annual averaged column AOD at 550 nm from (a) MODIS aboard the Aqua satellite (2003-2010); (b) CAM5 simulation averaged from 2001 to 2010.

Deleted: Page Break

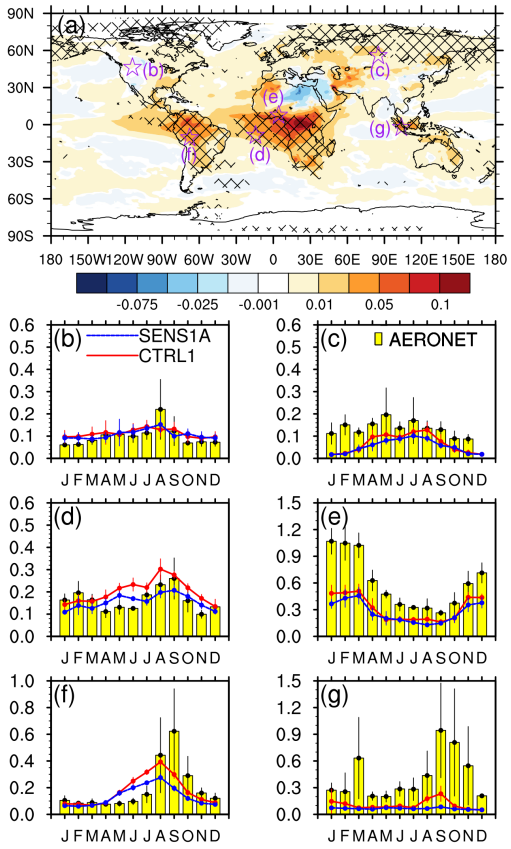

Deleted:

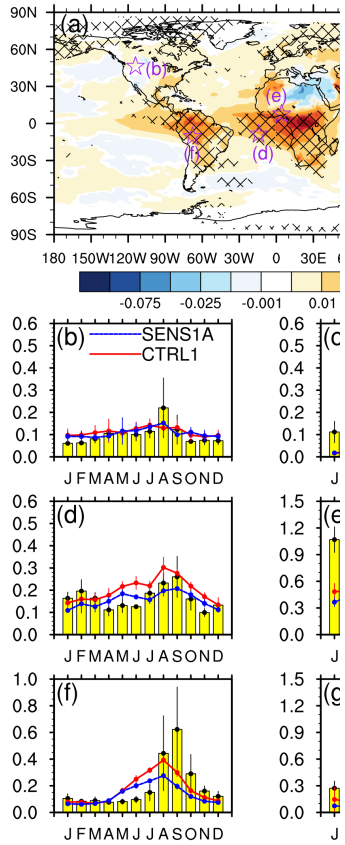

Deleted: in situ

240

1241 **Figure 2: CESM-RESFire simulation of (a) annual averaged fire contributed AOD at 550 nm (shading) in the present-day**
1242 **scenario (CTRL1-SENS1A). The stars denote the AERONET site location and the net meshes denote the 0.05 significance**
1243 **level of the two-tailed Student's t-test; (b) comparison with AERONET monthly AOT observations at 550 nm in Missoula**
1244 **(114.1°W, 46.9°N) during the 2000s. The error bars denote ±1 standard deviations of interannual variations in the**
1245 **simulations and observations, respectively.; (c) same as (b) but in Tomsk (85.1°E, 56.5°N); (d) same as (b) but in Ascension**
1246 **island (14.4°W, 8.0°S); (e) same as (b) but in Ilorin (4.3°E, 8.3°N); (f) same as (b) but in Rio Branco (67.9°W, 10.0°S); (g)**
1247 **same as (b) but in Jambi (103.6°E, 1.6°S).**

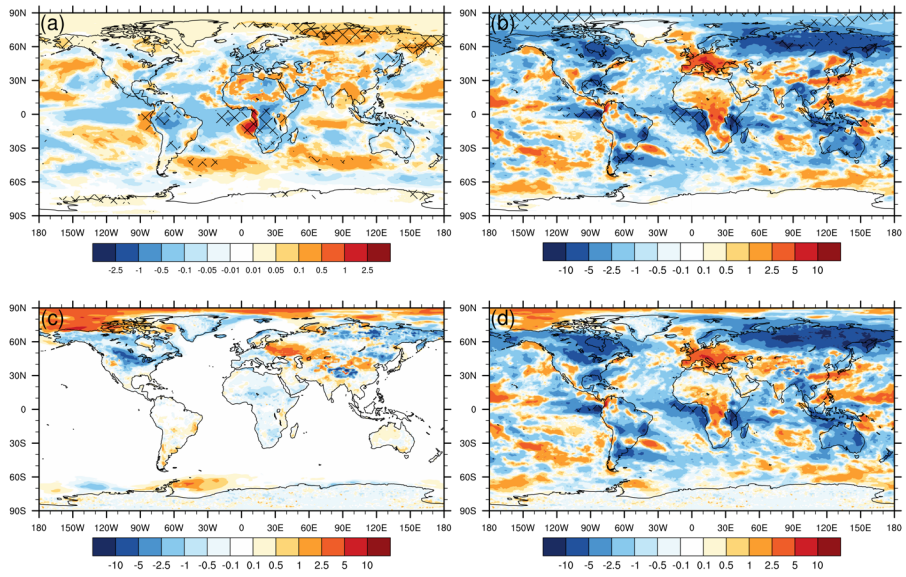

Figure 3: Present-day simulation of fire contributed annual averaged radiative effects through (a) aerosol-radiation interactions (RE_{ari}, W m^{-2}); (b) aerosol-cloud interactions (RE_{aci}, W m^{-2}); (c) fire aerosol-induced surface albedo change (RE_{sac}, W m^{-2}); (d) fire aerosol-related net radiative effects (RE_{aer}, W m^{-2}). All these radiative effects are estimated as changes in the shortwave radiative flux at the TOA between CTRL1 and SENS1A experiments. The net meshes denote the 0.05 significance level.

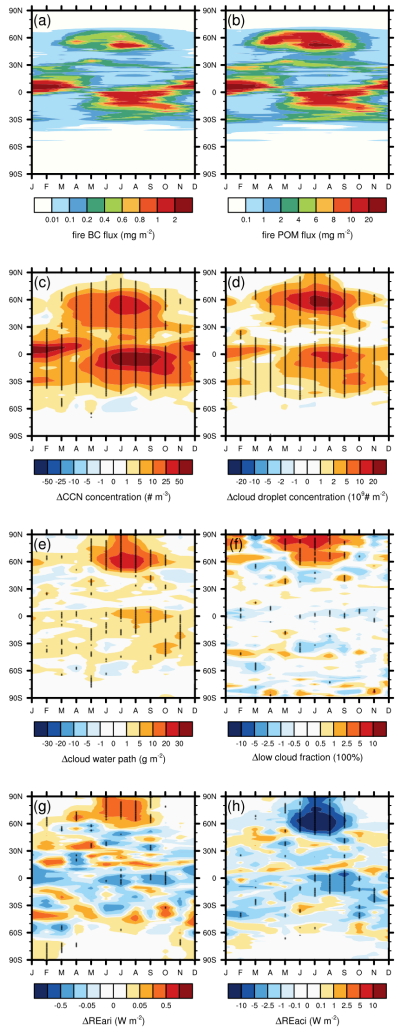

Figure 4: Present-day simulation of zonal averaged time-latitude cross sections of (a) monthly BC fire emission fluxes (mg m^{-2}) in CTRL1; (b) monthly POM fire emission fluxes (mg m^{-2}) in CTRL1; (c) fire-induced low-level (averaged below 800 hPa) cloud condensation nuclei (CCN, # m^{-3}) concentration changes (CTRL1-SENS1A); (d) vertically-integrated cloud droplet number concentration (CDNUMC, 10^9# m^{-2}) changes (CTRL1-SENS1A); (e) cloud water path (CWP, g m^{-2}) changes (CTRL1-SENS1A); (f) low cloud cover fraction (100%) changes (CTRL1-SENS1A); (g) radiative effect changes (CTRL1-SENS1A) by fire aerosol-radiation interactions (RE_{ari}, W m^{-2}); (h) radiative effect changes (CTRL1-SENS1A) by fire aerosol-cloud interactions (RE_{aci}, W m^{-2}). The dots in (c)-(h) denote the 0.05 significance level.

Deleted: 3

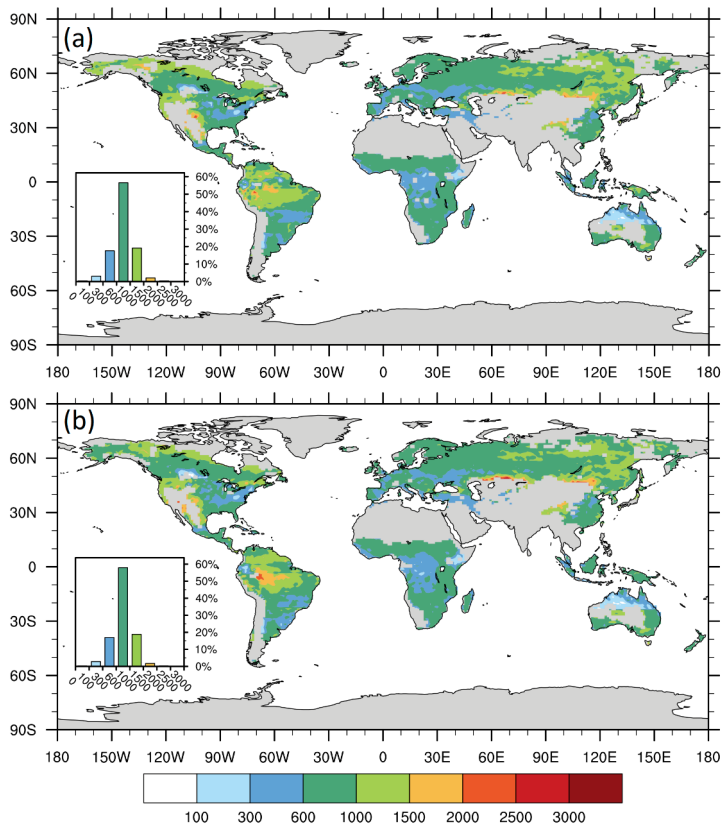

Figure 5: Comparison of CESM-RESFire simulated annual median injection heights (m) of fire plumes in the (a) present-day (CTRL1) and (b) RCP4.5 (CTRL2) scenarios. The inlets show statistical distributions of all plume injection heights in model grid cells of each scenario.

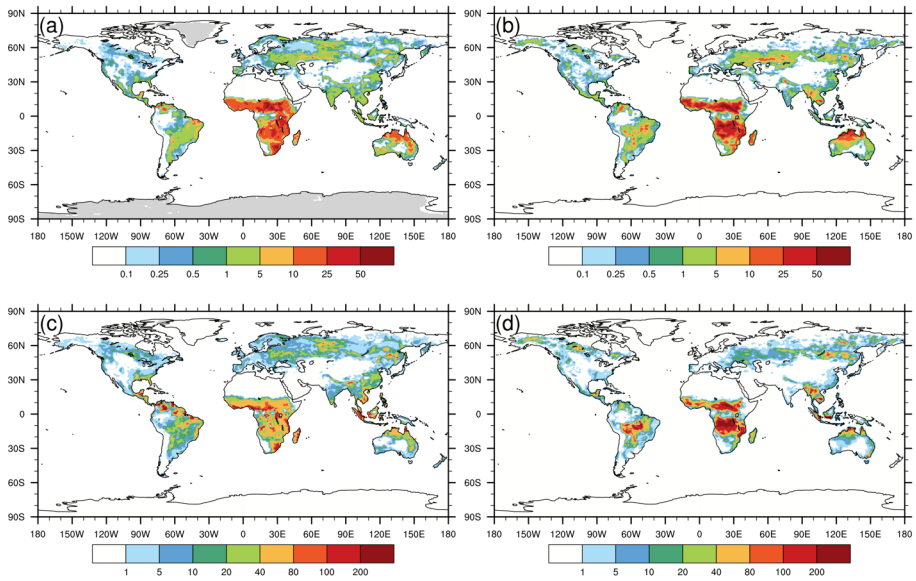

Figure 6: Comparison of CESM-RESFire simulations and GFED4.1s data. (a) ensemble averaged annual fractional burned area (% yr^{-1}) simulation; (b) 10-year averaged (2001-2010) annual fractional burned area (% yr^{-1}) based on the GFED4.1s data; (c) ensemble averaged annual fire carbon emission (gC m^{-2} yr^{-1}) simulation; (d) 10-year averaged (2001-2010) annual fire carbon emission (gC m^{-2} yr^{-1}) based on the GFED4.1s data.

Deleted: (%)

Deleted: (%)

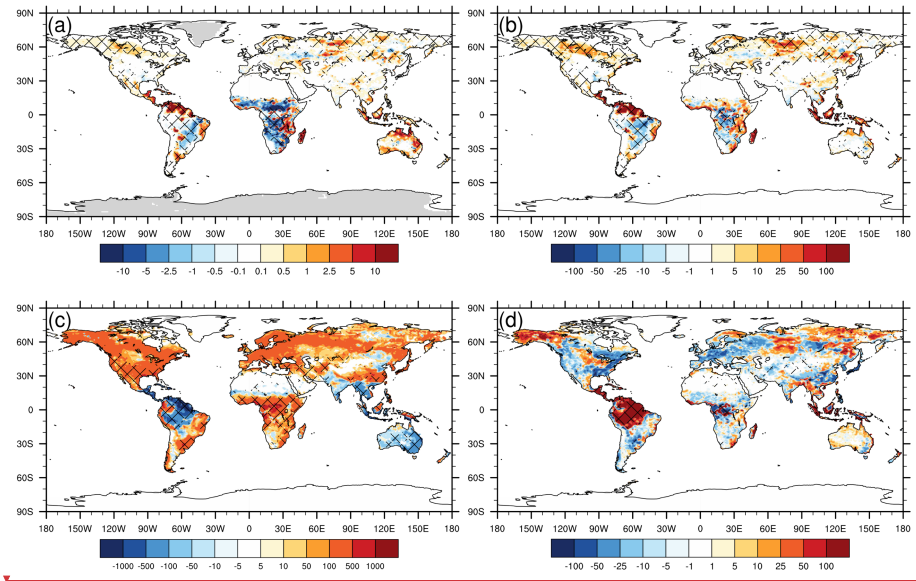

Figure 7: CESM-RESFire simulated changes between the RCP4.5 future scenario and the present-day scenario (CTRL2-CTRL1) in (a) annual fractional burned area (% yr^{-1}); (b) annual averaged fire carbon emissions (gC m^{-2} yr^{-1}); (c) annual averaged GPP (gC m^{-2} yr^{-1}); (d) annual averaged NEE (gC m^{-2} yr^{-1}). The net meshes denote the 0.05 significance level.

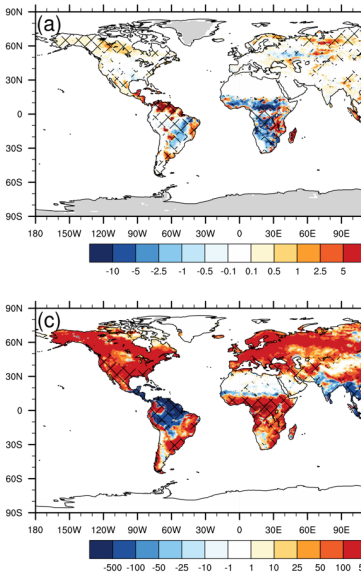

Deleted:

Deleted: areas (%);

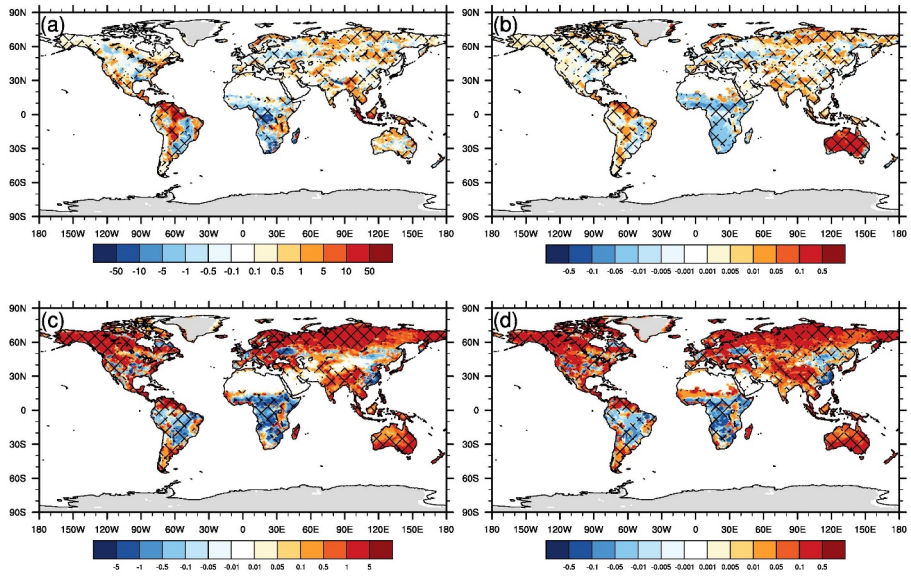

Figure 8: CESM-RESFire simulated changes in fire-related variables between the RCP4.5 future scenario and the present-day scenario (CTRL2-CTRL1). (a) changes in annual total fire ignition (NFIRE, 1E-3 count km^{-2} yr^{-1}); (b) changes in annual averaged fire combustion factors (FCF, unitless); (c) changes in annual averaged fire spread rates (FSR_DW, cm s^{-1}); (d) changes in annual averaged fire spread factors (FSF, unitless). The net meshes denote the 0.05 significance level.

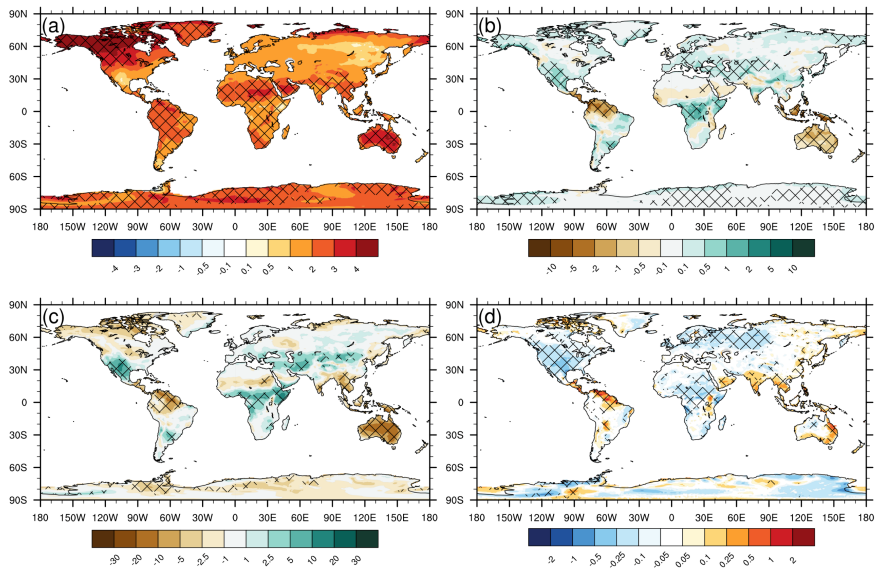

Figure 9: CESM-RESFire simulated changes in fire weather variables between the RCP4.5 future scenario and the present-day scenario (CTRL2-CTRL1). (a) changes in surface temperature (K); (b) changes in total precipitation rate (mm day^{-1}); (c) changes in surface relative humidity (%); (d) changes in surface wind speed (m s^{-1}). The net meshes denote the 0.05 significance level. For clear comparison with fire changes in Fig. 7 and 8, only fire weather changes over land are shown.

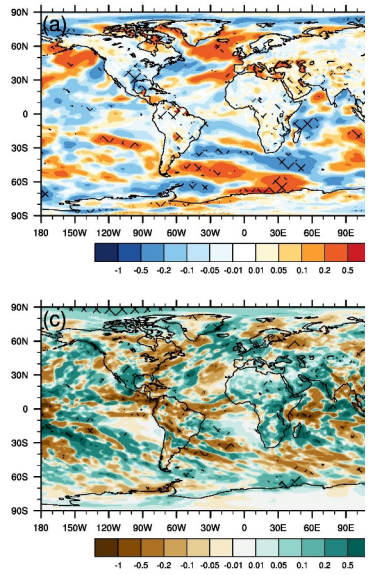

Deleted:

Deleted: wind speed (m s^{-1}); (b) changes in surface

Deleted: c

Deleted: rain

Deleted: snow precipitation (mm day

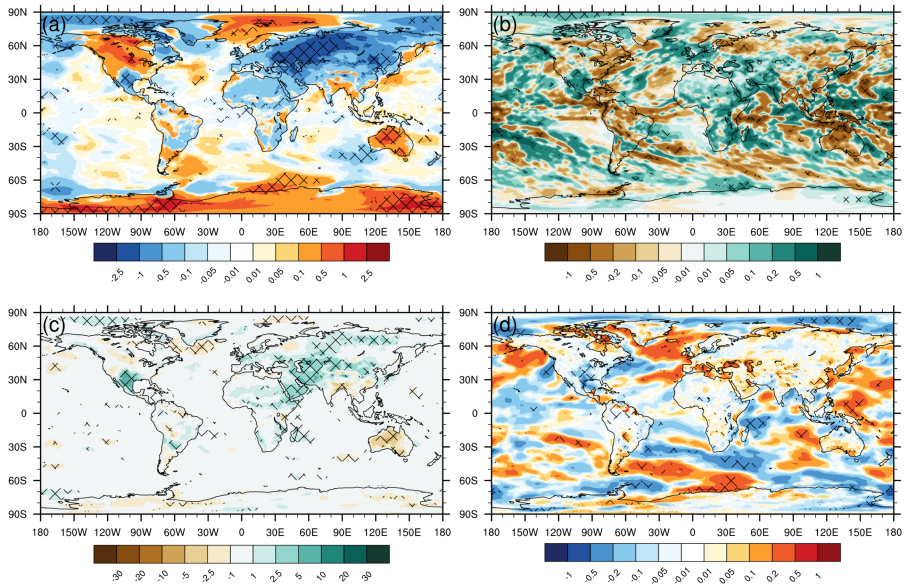

Figure 10: Fire induced changes in fire weather variables between the RCP4.5 future scenario and the present-day scenario ((CTRL2-CTRL1)-(SENS2B-SENS1B)). (a) fire induced changes in surface temperature (K); (b) fire induced changes in total precipitation rate (mm day^{-1}); (c) fire induced changes in surface relative humidity (%); (d) fire induced changes in surface wind speed (m s^{-1}). The net meshes denote the significance level of p=0.05.

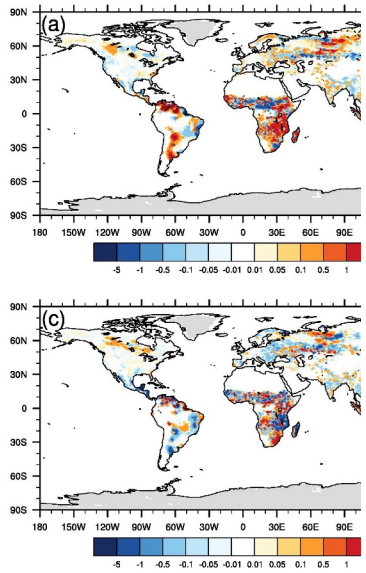

Deleted:

Deleted: Comparison of climate-fire-ecosystem interactions in CESM-RESFire sensitivity experiments in the RCP4.5 future scenario. (a) differences of annual total burned areas (%) between fire emission sensitivity experiments (CTRL2-SENS2A); (b) same as (a) but for differences of precipitation rates (mm day^{-1}); (c) differences of annual total burned areas (%) between fire-

Deleted: land cover change sensitivity experiments (SENS2A-SENS2B); (d) same as (c) but for differences of annual averaged fuel loads (gC m^{-2}). The net meshes denote the 0.05 significance level. ¶ ... [2]

Deleted: of

Deleted: aerosol-related climate

Deleted: (CTRL2-SENS2A)

Deleted: (CTRL1-SENS1A).

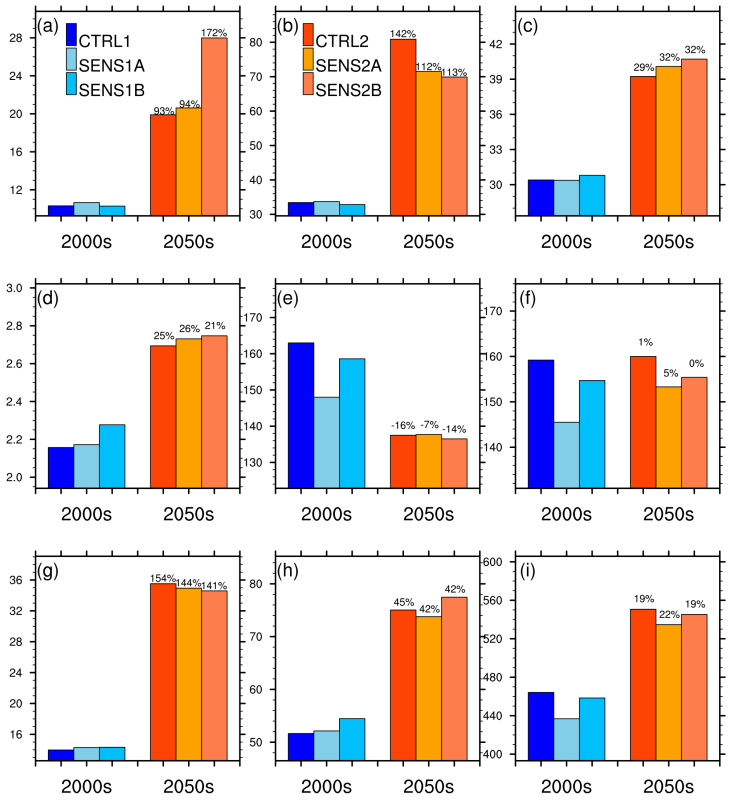

Figure 11: Comparison of annual burned area (Mha yr^{-1}) in each region among different time periods and sensitivity experiments. (a) North America; (b) South America; (c) Eurasia excluding Middle East and South Asia; (d) Middle East and North Africa; (e) Northern Hemisphere Africa; (f) Southern Hemisphere Africa; (g) South and Southeast Asia; (h) Oceania; (i) global total BA. The percentage numbers above projection columns are changes of burned area in the 2050s relative to their counterpart experiments in the 2000s. The spatial distributions of these regions are shown in Fig. S4 of the Supplement.

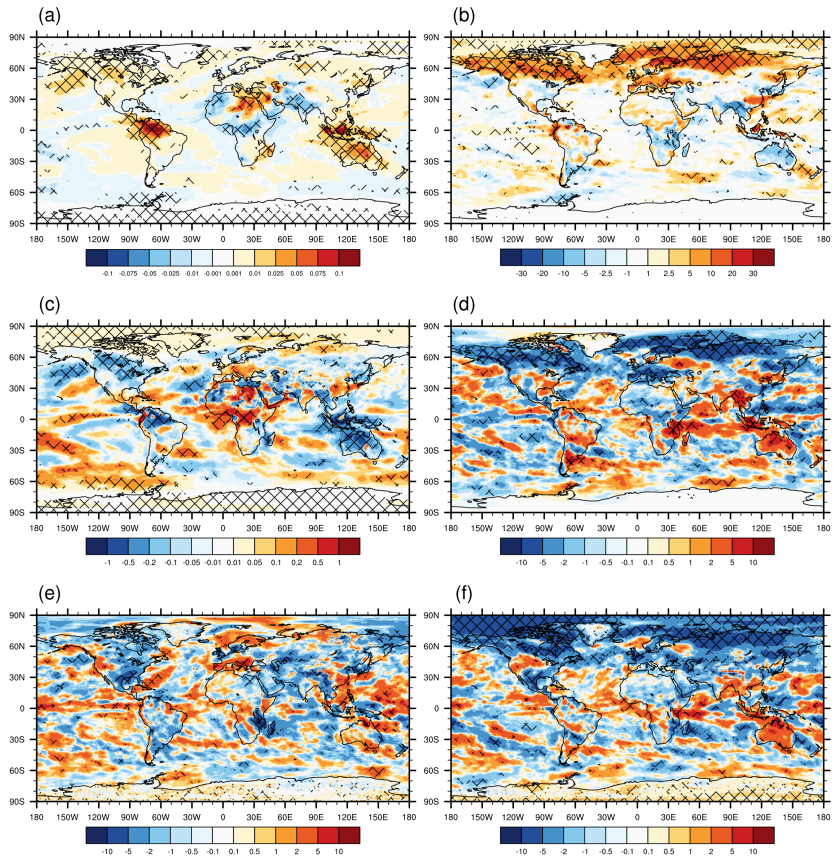

Figure 12: Changes in fire induced weather conditions and climate radiative forcing between the RCP4.5 future scenario and the present-day scenario. (a) changes in annual averaged column AOD at 550 nm (unitless, (CTRL2-SENS2A)-(CTRL1-SENS1A)); (b) changes in cloud liquid water path (g m^{-2}, (CTRL2-SENS2A)- (CTRL1-SENS1A)); (c) changes in RE_{ari} (W m^{-2}, (CTRL2-SENS2A)- (CTRL1-SENS1A)); (d) changes in RE_{aci} (W m^{-2}, (CTRL2-SENS2A)- (CTRL1-SENS1A)); (e) changes in RE_{lce} (W m^{-2}, (SENS2A-SENS2B)- (SENS1A-SENS1B)); (f) changes in RE_{fire} (W m^{-2}, (CTRL2-SENS2B)-(CTRL1-SENS1B)). The net meshes denote the 0.05 significance level.

Deleted:);

Deleted: CWP

Deleted:);

Deleted:);

Deleted:).

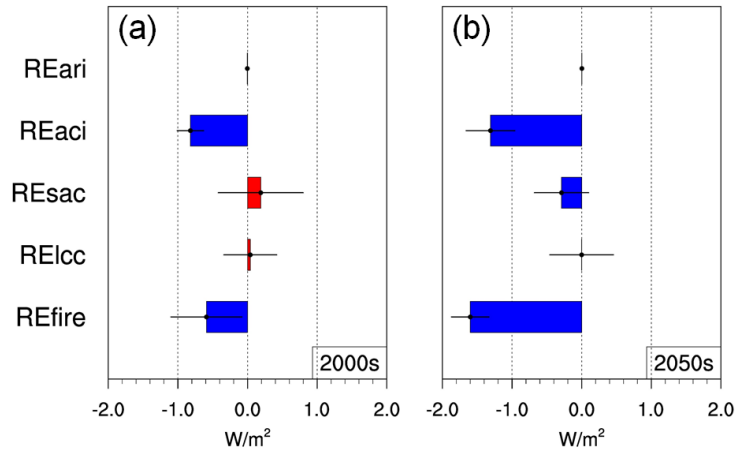

Figure 13: Comparison of CESM-RESFire simulated fire radiative effects (W m^{-2}) in (a) the present-day scenario and (b) the RCP4.5 future scenario. The error bars denote standard deviations of interannual variations during each 10-year simulation period.

Deleted: Page Break

Formatted: Font: 9 pt, Bold

Table 1: Fire sensitivity simulation experiments for the present-day and RCP4.5 future scenarios

Scenario	Present-day (2000)			Future (RCP4.5)		
Name	CTRL1	SENS1A	SENS1B	CTRL2	SENS2A	SENS2B
Time	2001-2010	2001-2010	2001-2010	2051-2060	2051-2060	2051-2060
Atmosphere	CAM5	CAM5	CAM5	CAM5	CAM5	CAM5
Land	CLM4.5	CLM4.5	CLM4.5	CLM4.5	CLM4.5	CLM4.5
Ocean	Climatology	Climatology	Climatology	RCP4.5 data	RCP4.5 data	RCP4.5 data
Sea ice	Climatology	Climatology	Climatology	RCP4.5 data	RCP4.5 data	RCP4.5 data
Non-fire emissions	IPCC AR5 emission data	IPCC AR5 emission data	IPCC AR5 emission data	RCP4.5 data	RCP4.5 data	RCP4.5 data
Fire emissions	Online fire aerosols with plume rise	–	–	Online fire aerosols with plume rise	–	–
Land cover	Fire disturbance on present-day conditions	Fire disturbance on present-day conditions	Fixed present-day conditions in 2000	Fire disturbance on RCP4.5 conditions	Fire disturbance on RCP4.5 conditions	Fixed RCP4.5 conditions in 2050

Formatted: Left, Line spacing: single

Table 2: Comparison of fire-related radiative effects in the present-day (CTRL1-SENS1A) and RCP4.5 future (CTRL2-SENS2A) scenarios based on this work and previous studies

Unit: W m^{-2}	This work		Jiang et al. (2016)	Ward et al. (2012)	
Time	2000s	2050s	2000s	2000s (CLM3/GFEDv2)	2100s (CCSM/ECHAM)
RE_{ari}	-0.003±0.013*	0.003±0.033	0.16±0.01	0.10/0.13	0.12/0.25
RE_{aci}	-0.82±0.19	-1.31±0.35	-0.70±0.05	-1.00/-1.64	-1.42/-1.74
RE_{sac}	0.19±0.61	-0.29±0.39	0.03±0.10	0.00/0.01	0.00/0.00
RE_{aer}	-0.64±0.48	-1.59±0.33	-0.55±0.07	-0.90/-1.50	-1.30/-1.49
RE_{lcc}	0.04±0.38	-0.006±0.457	—	-0.20/-0.11	-0.23/-0.29
RE_{fire}	-0.59±0.51	-1.60±0.27	-0.55±0.07	-0.55**/—	-0.83/-0.87**

*: the numbers after ± denote standard deviations of interannual variations;

**: the net radiative forcing includes other effects such as GHGs and climate-BGC feedback;

Table 3. Comparison of fire and carbon budget variables between CESM-RESFire simulations and previous studies and benchmarks

Variables	Time Period	This work		CLM-LL2013 (Li et al., 2014)	Benchmark	Sources
Models		RESFire-CRUNCEP	RESFire-CAM5c	CLM4.5-DATM		
Burned area (Mha yr^{-1})	1997-2004	508 ± 15	472 ± 14	322	510 ± 27	GFED4.1s (Giglio et al., 2013; Randerson et al., 2012)
Fire carbon emissions (Pg C yr^{-1})	1997-2004	2.3 ± 0.2	2.6 ± 0.1	2.1	2.2 ± 0.4	GFED4.1s (van der Werf et al., 2017)
NEE (Pg C yr^{-1})	1990s	-2.6 ± 0.6	-2.0 ± 1.3	-0.8	-1.1 ± 0.9 -2.0 ± 0.8	IPCC AR5 (Ciais et al., 2013) 10 models average (Piao et al., 2013)
GPP (Pg C yr^{-1})	2000-2004	142 ± 2	142 ± 1	130	133 ± 15	10 models average (Piao et al., 2013)
NPP (Pg C yr^{-1})	2000-2004	62 ± 1	63 ± 0.7	54	54	Zhao and Running (2010)

Deleted: ¶

Table 4. Comparison of carbon budget variables between the CRUNCEP data atmosphere driven fire simulations based on CESM-RESFire and CLM-LL2013

Variables	CESM-RESFire			CLM-LL2013 (Li et al., 2014)		
Unit: Pg C yr^{-1}	ΔFire	Fire on	Fire off	ΔFire	Fire on	Fire off
NEE	1.58	-2.67	-4.25	1.0	-0.1	-1.1
C_{fe}	2.08	2.08	0.0	1.9	1.9	0.0
$-NEP+C_{lh}$	-0.5	-4.75	-4.25	-0.9	-2.0	-1.1
NEP	0.5	4.8	4.3	0.8	3.0	2.3
NPP	0.4	61.7	61.3	-1.9	49.6	51.6
Rh	-0.1	56.9	57.0	-2.7	46.6	49.3
GPP	-0.1	142.3	142.4	-5.0	118.9	123.9
Ra	-0.5	80.6	81.1	-3.1	69.3	72.4
C_{lh}	0.0	0.05	0.05	-0.1	1.0	1.1

Table 5. Comparison of carbon budget variables between CESM-RESFire sensitivity experiments and previous studies

Variables	This work						Kloster et al. (2010) Kloster et al. (2012)	
Time (scenario)	2000s (CTRL1)	2050s (CTRL2)	2000s (SENS1A)	2050s (SENS2A)	2000s (SENS1B)	2050s (SENS2B)	2000s	2050s
Burned area (Mha yr^{-1})	464±19	551±16 (↑19%)*	437±17 (↓6%)**	535±19 (↓3%)	458±18 (↓1%)	545±18 (↓1%)	176-330	–
Fire carbon emissions (Pg C yr^{-1})	2.5±0.1	5.0±0.3 (↑100%)	–	–	–	–	2.0-2.4	2.7/ 3.4
GPP (Pg C yr^{-1})	141±1.2	146±1.1 (↑4%)	143±1.0 (↑1%)	149±1.3 (↑2%)	142±1.5 (↑1%)	150±1.3 (↑3%)	–	–
NEP (Pg C yr^{-1})	1.4±0.04	1.5±0.04 (↑7%)	1.4±0.04 (→0%)	1.6±0.04 (↑7%)	1.4±0.02 (→0%)	1.6±0.05 (↑7%)	–	–
NEE (Pg C yr^{-1})	1.2±0.03	1.6±0.05 (↑33%)	1.2±0.02 (→0%)	1.6±0.05 (→0%)	1.2±0.02 (→0%)	1.6±0.05 (→0%)	–	–

*: percentage numbers in the parentheses under CTRL2 denote relative changes comparing with the CTRL1 scenario.

**: percentage numbers in the parentheses under SENSx (x=1 or 2) denote relative changes comparing with the corresponding CTRLx (x=1 or 2) scenarios.

Page 12: [1] Deleted	**Zou, Yufei**	**12/6/19 1:40:00 PM**

Page 35: [2] Deleted	**Zou, Yufei**	**12/6/19 1:40:00 PM**